Optimization of Clamp Numbers and Positions to Mitigate Flow-Induced Vibration in High-Speed Fluid Flow Through a Pipe Elbow

Submitted By

Hasin Ahmad Zafir

190012117

Arafat Ahmed

190011104

Tanvir Hossain

190011111

Supervised By

Prof. Dr. Md. Zahid Hossain

A Thesis submitted in partial fulfillment of the requirement for the degrees of
Bachelor of Science in Industrial and Production Engineering
and
Bachelor of Science in Mechanical Engineering

Department of Mechanical and Production Engineering (MPE)

Islamic University of Technology (IUT)

June, 2024

Candidate's Declaration

This is to certify that the work presented in this thesis, titled, "Optimization of Clamp Numbers and Positions to Mitigate Flow-Induced Vibration in High-Speed Fluid Flow Through a Pipe Elbow", is the outcome of the investigation and research carried out by me under the supervision of Dr. Md. Zahid Hossain, Professor, Department of Mechanical and Production Engineering, Islamic University of Technology.

It is also declared that neither this thesis nor any part of it has been submitted elsewhere for the award of any degree or diploma.

Name of the Student
Student No: 190012117

Name of the Student
Student No: 190011104

Name of the Student
Student No: 190011111

Recommendation of the Thesis Supervisors

The thesis titled "Optimization of Clamp Numbers and Positions to Mitigate Flow-Induced Vibration in High-Speed Fluid Flow Through a Pipe Elbow" submitted by Hasin Ahmad Zafir, Student No: 190012117, Arafat Ahmed, Student No: 190011104, and Tanvir Hossain, Student No: 190011111; has been accepted as satisfactory in partial fulfillment of the requirements for the degree of B Sc. in Mechanical Engineering **on 21st June, 2024.**

1. ----------

Dr. Md. Zahid Hossain (Supervisor)
Professor
MPE Dept., IUT, Board Bazar, Gazipur-1704, Bangladesh.

CO-PO Mapping of ME 4800 -Theis and Project

COs	Course Outcomes (CO) Statement	(PO)	Addressed by	
CO1	Discover and Locate research problems and illustrate them via figures/tables or projections/ideas through field visit and literature review and determine/Setting aim and objectives of the project/work/research in specific, measurable, achievable, realistic and timeframe manner.	**PO2**	Thesis Book	
			Performance by research	
			Presentation and soft skill	
CO2	Design research solutions of the problems towards achieving the objectives and its application. Design systems, components or processes that meets related needs in the field of mechanical engineering	**PO3**	Thesis Book	
			Performance by research	
			Presentation and soft skill	
CO3	Review, debate, compare and contrast the relevant literature contents. Relevance of this research/study. Methods, tools, and techniques used by past researchers and justification of use of them in this work.	**PO4**	Thesis Book	
			Performance by research	
			Presentation and soft skill	
CO4	Analyse data and exhibit results using tables, diagrams, graphs with their interpretation. Investigate the designed solutions to solve the problems through case study/survey study/experimentation/simulation using modern tools and techniques.	**PO5**	Thesis Book	
			Performance by research	
			Presentation and soft skill	
CO5	Apply outcome of the study to assess societal, health, safety, legal and cultural issue and consequent possibilities relevant to mechanical engineering practice.	**PO6**	Thesis Book	
			Performance by research	
			Presentation and soft skill	
CO6	Relate the solution/s to objectives of the research/work for improving desired performances including economic, social and environmental benefits.	**PO7**	Thesis Book	
			Performance by research	
			Presentation and soft skill	
CO7	Apply moral values and research/professional ethics throughout the work, and justify to genuine referencing on sources, and demonstration of own contribution.	**PO8**	Thesis Book	
			Performance by research	
			Presentation and soft skill	
CO8	Perform own self and manage group activities from the beginning to the end of the research/work as a quality work.	**PO9**	Thesis Book	
			Performance by research	
			Presentation and soft skill	
CO9	Compile and arrange the work outputs, write the report/thesis, a sample journal paper, and present the work to wider audience using modern communication tools and techniques.	**PO10**	Thesis Book	
			Performance by research	
			Presentation and soft skill	
CO10	Organize and control cost and time of the work/project/research and coordinate them until the end of it.	**PO11**	Thesis Book	
			Performance by research	
			Presentation and soft skill	
CO11	Recognize the necessity of life-long learning in career development in dynamic real-world situations from the experience of completing this project.	**PO12**	Thesis Book	
			Performance by research	
			Presentation and soft skill	

Student Name /ID:

1……..

2. ……..

3. ……..

Signature of the Supervisor: ……

Name of the Supervisor: ……..

K-P-A Mapping of ME 4800 -Theis and Project

COs	POs	Related Ks								Related Ps							Related As				
		K1	K2	K3	K4	K5	K6	K7	K8	P1	P2	P3	P4	P5	P6	P7	A1	A2	A3	A4	A5
CO1	PO2	☒	☐	☒	☒	☒	☒	☒	☒	☒	☒	☐	☒	☐	☐	☒	☐	☒	☒	☐	☒
CO2	PO3	☐	☐	☒	☒	☒	☒	☒	☒	☒	☒	☐	☒	☐	☐	☒	☐	☒	☒	☐	☒
CO3	PO4	☒	☐	☒	☒	☒	☒	☒	☒	☒	☒	☐	☒	☐	☐	☒	☐	☐	☒	☐	☒
CO4	PO5	☒	☐	☐	☒	☒	☒	☒	☒	☒	☒	☐	☒	☐	☐	☒	☐	☐	☒	☐	☒
CO5	PO6	☐	☐	☐	☐	☐	☐	☐	☐	☐	☐	☐	☐	☐	☐	☐	☐	☐	☐	☐	☐
CO6	PO6	☐	☐	☐	☐	☐	☐	☐	☐	☐	☐	☐	☐	☐	☐	☐	☐	☐	☐	☐	☐
CO7	PO8	☐	☐	☐	☐	☐	☐	☐	☐	☐	☐	☐	☐	☐	☐	☐	☐	☐	☐	☐	☐
CO8	PO9	☐	☒	☐	☐	☐	☐	☐	☐	☐	☒	☐	☒	☐	☐	☐	☒	☐	☐	☒	☐
CO9	PO10	☒	☐	☒	☒	☒	☒	☒	☐	☒	☒	☒	☐	☒	☐	☒	☐	☐	☒	☐	☒
CO10	PO11	☐	☐	☐	☐	☐	☐	☐	☐	☐	☐	☐	☐	☐	☐	☐	☐	☐	☐	☐	☐
CO11	PO12	☐	☐	☒	☒	☒	☒	☒	☐	☒	☒	☒	☐	☒	☐	☒	☐	☐	☒	☐	☒

Student Name /ID:

1……..

2. ……..

3. ……..

Signature of the Supervisor: ……

Name of the Supervisor: ……..

Acknowledgment

This work is done through the grace and guidance of the Almighty.

A heartfelt gratitude goes to our parents and honorable supervisor Professor Dr. Md Zahid Hossain sir for their unending support throughout the study.

Special thanks to Dr. Ahmed A Abuhatira CEng IMechE MIET FHEA, Lecturer and Researcher, Lakes College West Cambria for his help during the validation process.

Abstract

Vibration in pipe systems can cause fatigue failure, cracking, and life cycle reduction. This paper aims to mitigate flow-induced vibration (FIV) in a pipeline system by finding optimal clamping locations and numbers through simulation. The simulation is based on one-way Fluid-Structure Interaction (FSI) methodology. The goal is to obtain the vibration signal in the form of acceleration in the time domain and then analyze it in the frequency domain to find amplitudes of concern. Previous investigations on the analysis of clamp locations based on vibration-damping characteristics have been proven to be time-consuming and inaccurate. This project aims to use the Ansys Workbench to perform the numerical analysis of fluid passing through a 90-degree pipe elbow by integrating Computational Fluid Dynamics (CFD) with the Finite Element Analysis (FEA). The study also outlines a workflow to use the acceleration data from the FEA to analyze the vibration-damping properties of a standard clamp suitable for the chosen pipe parameters. The clamp locations are optimized by analyzing 15 different possible locations and the number of clamps is optimized by analyzing the vibration and displacement of the pipe during fluid flow. Two optimal clamp locations were found for a chosen pipe segment. This process gives an insight into a quick and accurate way of optimizing clamp locations and numbers based on their effect on the vibration of a complex pipeline system.

Keywords: FIV reduction, Pipe flow, FSI, Superheated Steam, Clamping, Vibration mitigation

Table of Contents

List of Figures

List of Tables

Nomenclatures and Symbol

Abbreviation	Meaning
FIV	Flow-Induced Vibration
AIV	Acoustic-Induced Vibration
ASD	Adjustable Speed Drive
NTSB	National Transportation Safety Board
LSV	Laser Doppler Vibrometry
CFD	Computational Fluid Dynamics
FSI	Fluid-Structure Interaction
FEA	Finite Element Analysis
RANS	Reynolds Average Navier Stokes
LES	Large Eddy Simulation
RSM	Reynolds Stress Model
FT	Fourier Transform
DFT	Discrete Fourier Transform
FFT	Fast Fourier Transform
CAD	Computer-Aided Design
SCH	Schedule
BS	Baseline System
LS	Leak Sensitivity

List of symbols:

n = number of data sets

μ = dynamic viscosity

Chapter 1: Introduction

1.1 What is Mechanical Vibration?

Mechanical vibrations are the oscillatory or repetitive motions of a mechanical system around an equilibrium position [1]. This involves a magnitude (such as force, displacement, or acceleration) that fluctuates around a specified reference point, with the magnitude alternately being smaller or larger than this reference. Vibration is typically measured in terms of frequency, represented in cycles per second or Hertz (Hz), and amplitude, which denotes the magnitude of the force, displacement, or acceleration [2].

1.2 Pipe Vibration

Pipe vibration is considered to be the alternating movement of the pipe structure due to the fluid passing through it [3]. Pipeline vibration in general is the result of quite a few factors. There's turbulent Flow Induced Vibration (FIV) resulting from flow discontinuities such as bends, and tees. The increased level of kinetic energy generated downstream usually converges at frequencies less than 100Hz [4] There's machinery-induced vibration where excessive pipe or compressor manifold system vibration levels generally develop when a mechanical natural frequency is excited by a pulsation or mechanical excitation source. Since reciprocating machinery generates large pulsation energy at various harmonics, major vibration issues in reciprocating machinery systems are typical [5]. There's Acoustic Induced Vibration (AIV) which refers to the high acoustic energy created by pressure-reducing devices that activate pipe shell vibration modes, causing excessive dynamic stress [6]. Acoustic vibration is defined as a sound, generally of a particular pitch ranging from a low rumble to a piercing scream.

1.3 What is Resonance?

Vibration resonance occurs when equipment or a product is subjected to an external force vibrating at one or more of its natural frequencies. This causes the product's response vibration to amplify significantly, which can be substantial. Vibration resonances can lead to severe damage to products and considerably reduce their lifespan [7]. In machinery like pumps, turbines, and electric motors, resonance can magnify the minor vibratory forces generated during operation, leading to severe vibration levels. Such issues often arise after a change in operating speed, such as when a machine is retrofitted with an adjustable-speed drive (ASD) or when a 50-hertz motor is operated on 60 hertz of power [8]. The solution is to avoid the critical frequencies when implementing external force.

1.4 Engineering Failures due to Vibration

To investigate the dangers of vibration, we need to look back at the 20th century particularly at the year 1940 when the 1st suspension bridge of the Tacoma region of Washington, US known as Takoma Bridge collapsed due to turbulent wind flowing over the bridge making the bridge vibrate randomly and dangerously [9]. The initial investigation concluded that the bridge was too flexible to withstand the randomness of the wind turbulence. More than 50 years later, the engineering world witnessed another major incident caused by vibration when a sodium-cooled fast reactor named Monju near the Tsuruga Nuclear Power Plant experience a sodium leak resulting in a major fire incident [10]. Based on the primary investigation, it is said that intense vibration caused the thermocouple inside the sodium coolant pipe to break thus enabling the

sodium to contact with air and caused fumes that broke the fire. Another major engineering failures due to resonance would likely be the failure of Broughton Suspension Bridge failure when the frequency of the marching band of soldiers matched with the natural frequency of the suspension bridge resulting in resonance phenomenon and vibrate excessively [11]. Another destructive phenomenon due to vibration is known as ground resonance, an instability that can occur when a helicopter is on the ground. It arises from the resonance between the oscillation of the main rotor and the helicopter's oscillation on its landing gear, often due to poor maintenance. The NTSB has documented 34 incidents of ground resonance in the US since 1990 [12].

1.5 Challenges due to Flow-Induced Vibration

Flow Induced Vibration also known as FIV is generally a low frequency (<100Hz) vibration typically consisting of a large amplitude usually occurs in pipelines carrying high inlet velocity turbulent fluids [13]. The high kinetic energy imparted by the flowing fluid causes the pipe to vibrate and it's mostly prevalent near the turbulent sources such as bends, valves, connections, reducers. The problem with FIV is that this kind of vibration causes the pipe to reciprocate in both longitudinal and transverse direction [14]. This in turn leads to damage in pipe supports and fatigue failure. And the UK Health & Safety Executive states that around 21% of global hydrocarbon releases are caused by vibration-induced fatigue failures [15]. The leading source of pipeline leakage is due to pipe vibration and the reason being the sheer quantity and complexity of the pipe network makes incorporating vibration parameters in design code much for difficult. Not only that, wear, fretting and excessive noise are also some of the unwanted phenomena generated by the pipe vibration caused by fluid flow.

Chapter 2: Literature Review

2.1 Vibration Detection Methods

Several researchers tried to find out how turbulent flow induces pipe vibration on the elbow of a 90-degree bent pipe. Researchers have categorized them into various groups: Experimental analysis, Numerical Simulation, Analytical Approaches. Over the last decade, various methods have been proposed and tested such as Laser Doppler Vibrometry (LSV) for non-contact vibration measurement [16], combined Finite Element Analysis and CFD to simulate structural responses of pipes to turbulent flow [17], Analytical models to generate predictive formulas for flow-induced vibration [18], Eigenvalue analysis for natural frequency determination [19], Machine learning model to analyze and predict turbulent flow induced vibration [20], Acoustic emission technique to detect high-frequency stress waves [21].

2.2 FSI Method for Vibration Detection

In this paper we tried to focus on the FSI based CFD analysis for vibration prediction. The interplay between the flexible structures and the surrounding fluid in known as Fluid Structure Interaction[22]. Solid structure deforms due to fluid pressure fluctuation caused by the flowing fluid. Structure then again creates a change in the flow regime causing further change in dynamic behaviour of the pipe and this process is iterative. This interaction is particularly useful when it comes to modelling and designing aircraft wing structures, turbomachine components, pipeline design etc.

Back in 1998 Païdoussis did a lot of research on dynamics of slender pipes containing flowing fluids [23]. Païdoussis especially focused on the dynamic behaviour of the curved pipes compared to the straight pipes under various flow conditions. And in 2005 he expanded his book by adding comprehensive knowledge on FSI modelling techniques using transfer matrix method and spectral element method for complicated pipeline networks.

Early research on developing theoretical models for FSI includes 4 equation model by Tijsseling et.al. [24] 6 equation model by Walker and Phillps [25], 8 equation model by Gale [26], 12 equation model by Shen [27] and 14 equation model by Lee [28] . In 2018, Zhao introduced a new transfer matrix method for vibration analysis of a curved pipe by incorporating Laplace transform for 3 different boundary conditions: cantilevered, clamped-elastically supported and periodic cantilevered curved pipes [29].

2.3 Two-Way Coupling vs One-Way Coupling

In the year 2011, Friedrich-Karl Benra tried to investigate the differences between one-way and two-way coupling based FSI simulations [30]. In his study, he found that the solution time for two-way coupling is three-four times more than one-way coupling simulation. He also denoted that deflection frequency is mostly the same if the vortex frequency is close to the natural frequency and thus one-way coupling is preferred in this case. But overall, two-way coupling provides the values close to the experimental data.

A recent study on FIV for both one-way and two-way coupling done by Kamal Haziq [31]showed fluid velocity impact on the dynamic behaviour of the structure in both cases. The author generated pressure and velocity distribution for both laminar and turbulent flows and also generated the modal frequencies using modal analysis. The study showed that two-way coupling showed little to no change in pipe deformation compared to one-way coupling. And thus, for our purpose, we opted with one-way coupling method.

2.4 RANS vs LES Model

Analytically investigating the solutions for the FSI problem requires many assumptions; thus, a numerical model provides a better insight into this phenomenon. The 1st FSI modelling was done by Saito et al. in 1990 to compare their experimental data. Saito imported the pressure measured from the experimental setup to the NASTRAN FEA model [32]. Many researchers followed continued the approach of Saito to model many complex flow-induced vibrations later on.

Most of the turbulence models used in commercial software packages use RANS equations as their basic governing equations. However, the problem with the RANS model is that it doesn't compute the pressure fluctuation at the fluid-structure interface and generates results based on average velocity and pressure. Here comes the Large Eddy Simulation (LES) model. The advantage of using the LES model is that LES computes the instantaneous fluctuations when it comes to turbulent flow and thus in 2003, Mattew T. Pittard used the LES method in his numerical model to investigate turbulent flow-induced pipe vibration [33]. Pittard's work showed that the instantaneous fluctuations of the turbulent flow do contribute to the pipe vibration. However, the downside of the LES model is the computation time. If the model is based on multiple structure domains, then it's best to opt for the RANS method.

There are different types of RANS-based turbulence models, namely k-ε, k-ω, and Reynolds Stress Model (RSM).

In 2006, P. R. Resende compared the performance of the k-ε model with the RSM model in turbulent flows for viscoelastic fluids [34]. His improved RSM model was based on a Newtonian Consecutive Equation that accounted for elastic effects. His model showed improved results where the linear and non-linear k-ε models underpredicted the levels of drag reduction.

In 2009, Sowjanya Vijiapurapu compared different RANS-based turbulent models for flow through rough pipes and showed that accurate quantitative calculations can be done with the least effort. [35]. The RSM method on the other hand is more time-consuming but provides information not only on the time-averaged flow statistics but also showcases the shear-stress correlations.

2.5 y+ Value

The wall y^+ refers to a non-dimensional distance similar to the local Reynolds Number. In terms of CFD, it refers to the coarseness or fineness of a mess for a particular flow[36]. In CFD, it's important to balance the reliable accuracy of the mesh with the time required.

Salim investigated the grid independence test using the wall y^+ method to determine the proper grid configuration and corresponding turbulent models [37]. Salim then compared it with the experimental data of Zeidan and determined that a wall y^+ at the low-law region for the range of 30-60 is sufficiently accurate.

Abuhatira conducted a numerical simulation of a 90-degree elbow wall based on Salim's work to establish a guide on using the wall y^+ approach to select an appropriate turbulence model [38]. In this work, he compared 4 different RANS models (RSM, k-e, k-e, SSM) on 3 different meshes i: e: $y^+ \approx 3$, $y^+ \approx 19$, $y^+ \approx 39$ using quantitative assessment R^2 and found that the RSM model on $y^+ \approx 3$ provides the highest accuracy in the simulation.

2.6 Fast Fourier Transform (FFT) Method

Fourier Transform operation transforms the data from the time domain to the frequency domain [39]. This method is widely used in vibration measurement techniques when the result data is in the time domain and needs to be converted into the frequency domain to check for the dynamic behavior of the structure for different frequencies. There are currently two different types of Fourier transform techniques available: Fourier Transform (FT) and discrete Fourier Transform (DFT).
In conventional FT, the algorithm takes continuous time domain signals and where the signal is periodic and discrete, DFT is used. Fast Fourier Transform (FFT) is an algorithm used in DFT to make the process faster and more efficient. FFT manages to transform the computational complexity of DFT from $O(n^2)$ to $O(nlogn)$ thus FFT algorithm is more useful for large datasets [40].

2.7 Relationship between Fluid Flow Characteristics and Pipe Dynamics

Pittard [41] first tried to investigate turbulent flow-induced pipe vibration using both experimental and numerical approaches. For the experimental method of pipe vibration detection, Pittard used an accelerometer for measure the standard deviation of the frequency-averaged time-series signal. For the numerical approach, Pittard used LES-based flow models that can compute instantaneous pressure fluctuations due to turbulent flow. Pittard's work showcased the strong relationship between the acceleration of the pipe and the flow rate. Pittard also showcased that pressure fluctuations near the wall were in a quadratic relationship with the pipe.
Abuhatira [42] used Reynolds Stress Model (RSM) as the flow model to investigate leak points in a bent pipe due to turbulent flow-induced pipe vibration. Abuhatira first determined the variation of the fluid behaviour such as certrifugal force, and pressure drop using one-way FSI coupling in CFD approach. He then imported the CFD results to the structural model and in turn measured vibration signals in terms of acceleration. Abuhatira in his work investigated for no leak and 5 different leak conditions on the pipe elbow and showcased the pressure and acceleration fluctuation concerning the inlet fluid(oil) velocity fluctuation.

2.8 Research Gaps

While the above-mentioned studies shed light on the effectiveness of FIV investigation of bent pipe using FSI method, it is to say that there are still gaps in the research literature for FSI-based FIV investigation for high-speed fluid (greater than 50 m/s) compared to existing literature flow, especially superheated steam used in industrial boilers. Subsequently, clamp properties, numbers and their positions' optimization modeling for a given parameters of a pipe network containing 90-degree elbow bends are very important for mitigating FIV.
In our paper, we have considered the computational modeling of FIV in a 90-degree pipe elbow from a steam power plant. FIV in normal conditions (no leak) has been investigated in our model. Based on the recommendation of Abuhatira, the study of the wall y^+ approach, the Reynolds Stress Model (RSM) is coupled with FEA to simulate the FSI using one-way coupling. We used the RSM turbulence model since the LES model, although more accurate, demands heavy computational power and longer simulation time. And since two-way coupling shows little to no change in pipe deformation compared to one-way coupling, we chose one-way coupling for our study. The RSM turbulence model of this paper and the FSI approach taken were initially validated against the no-leak condition of Abuhatira's paper.

2.9 Problem Formulation

Reviewing existing literature contributed to finding the main problem areas to focus on through this study. There was no significant work on vibration for high pressure (>10MPa), and high speed (>50m/s) fluid flow through pipe elbow. Furthermore, no investigation on superheated steam flow on complex industrial pipelines was found and there was an overall lack of clamp number and location optimization model

2.10 Objectives of this study

The main objectives of this study are-

- To generate a fluid pressure distribution graph of the fluid domain (superheated steam) using CFD analysis

- To investigate the acceleration and deformation of the pipe structure concerning time by importing the pressure distribution to the transient structure in transient analysis

- To optimize clamp numbers and positions based on the Fast Fourier Transform (FFT) of acceleration and deformation data of different mass flow rates.

Chapter 3: Description of the Model/System

Figure 1 presents the flowchart detailing the comprehensive workflow implemented in this study. The first stage involves identifying the problem and defining the research objectives. This was achieved through an extensive literature review, which helped identify the research gap and helped to set a clear direction for the study. After identifying the problem and objectives, the system design and parameter selection procedures are taken. This procedure involves both Fluid domain configuration and Structural domain configuration. The fluid domain configuration primarily focuses on analyzing the fluid characteristics due to the flow through the pipe, such as pressure distribution, velocity contour, etc. Then, this pressure data is imported into the structural domain to study the impact of acceleration and deformation on the structural domain. Data concerning accelerations and deformations is extracted and analyzed using Python, with techniques such as Fast Fourier Transform (FFT) for detailed vibrational analysis. The outcome of this comprehensive analysis assists in determining the optimal clamping positions.

This study used a comprehensive Fluid-Structure Interaction (FSI) analysis to find the best clamping position for a 90-degree bent pipe in a boiler's pipeline system. The main goal was to determine the optimal clamping position based on the distance from the pipe's elbow. This was

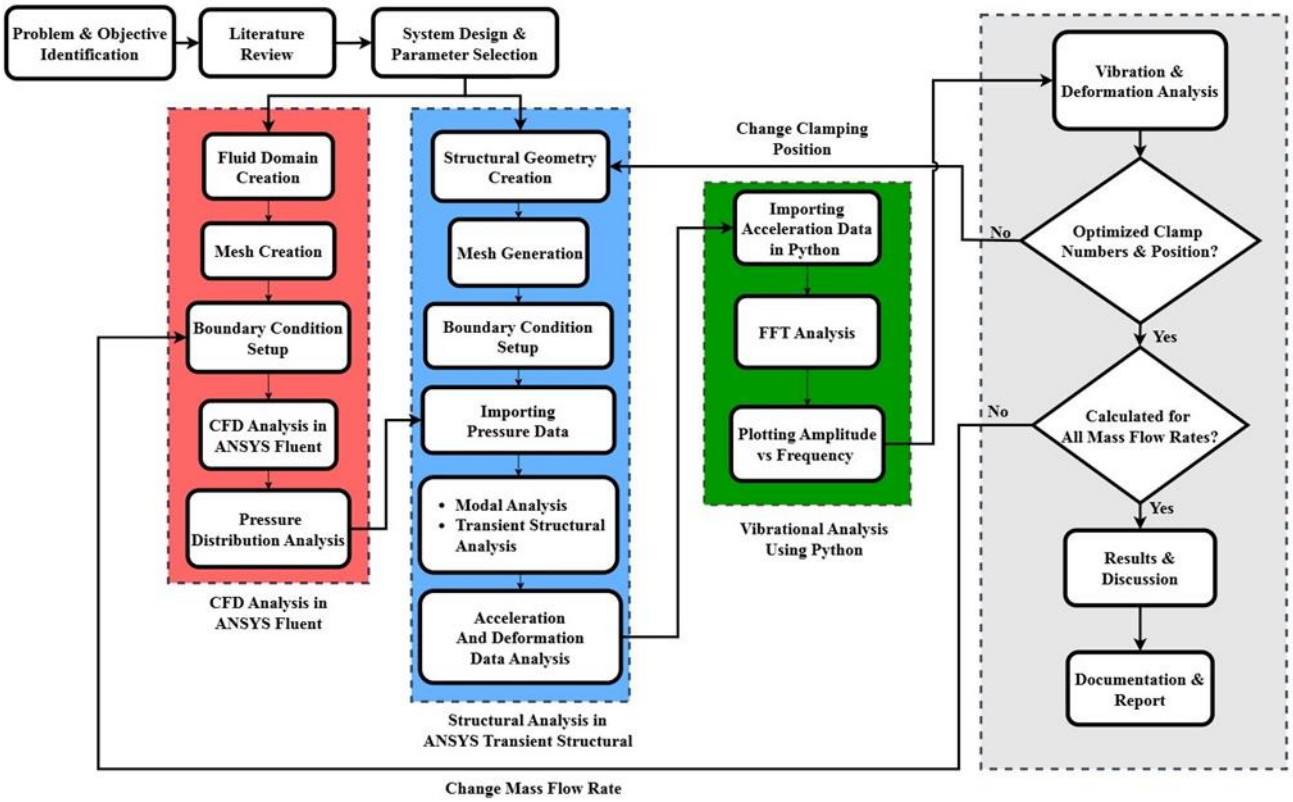

Figure 1: Methodology Flowchart

done to reduce vibration and deformation, lowering the risk of fatigue failure and increasing the overall lifespan of the piping system. The clamping position was determined through FSI analysis performed at different flow rates. The study conducted a strategic analysis of the dynamic behavior of the bent pipe under various clamping configurations.

Fluid-structure interaction (FSI) is a sophisticated computational method that models the interaction between fluid flow and structural deformation. FSI, or Fluid-Structure Interaction, combines Computational Fluid Dynamics (CFD) and Finite Element Analysis (FEA) to gain a thorough understanding of the integrated fluid-structure system [24]. The Fluid flow results from the CFD model are then imported into the structural model. This coupling method, used to diagnose any FSI, is defined as a one-way FSI [25]. In the one-way coupling method, it is considered that the effect of the change in structural deformations hardly affects the fluid domain. In this process, parameters like pressure distribution and fluid forces are obtained from the CFD analysis. The output from the CFD analysis, especially the pressure distribution and forces, are applied as external forces to the structural model. The simulation helps predict the pipe's behavior under various boundary conditions, such as different clamping positions, flow rates, materials, etc. Prior research has investigated Fluid-Structure Interaction (FSI) in other contexts, such as using vibrations to detect leaks and analyzing pipeline erosion [21] [25].

3.1 Structure Domain:

The subsequent phase of the study focuses on the structural domain and examines the vibrational response induced by pressure fluctuations within the internal pipe wall. A precise Finite Element Analysis (FEA) methodology calculates this vibrational response. This process includes creating the geometry in CAD software, which was then divided into smaller sections of the geometry. Specific material was assigned to all the sections, and boundary conditions were applied with a particular load imported from CFD analysis.

The structural domain under examination represents an intricate piping system segment designed to convey super-heated, high-speed steam within a power generation boiler. The inlet section of this system is directly connected to the boiler. For this application, a Schedule SCH 100 carbon steel pipe is utilized.

As shown in **Figure 2**, this section of the pipe encompasses an upstream length of 2 meters and a downstream length of 4 meters. The radius of curvature of the elbow is 0.57 m. Additionally, the pipe has a wall thickness of 0.026 meters and an inner radius of 0.354 meters, as shown in **Table 1** [21].

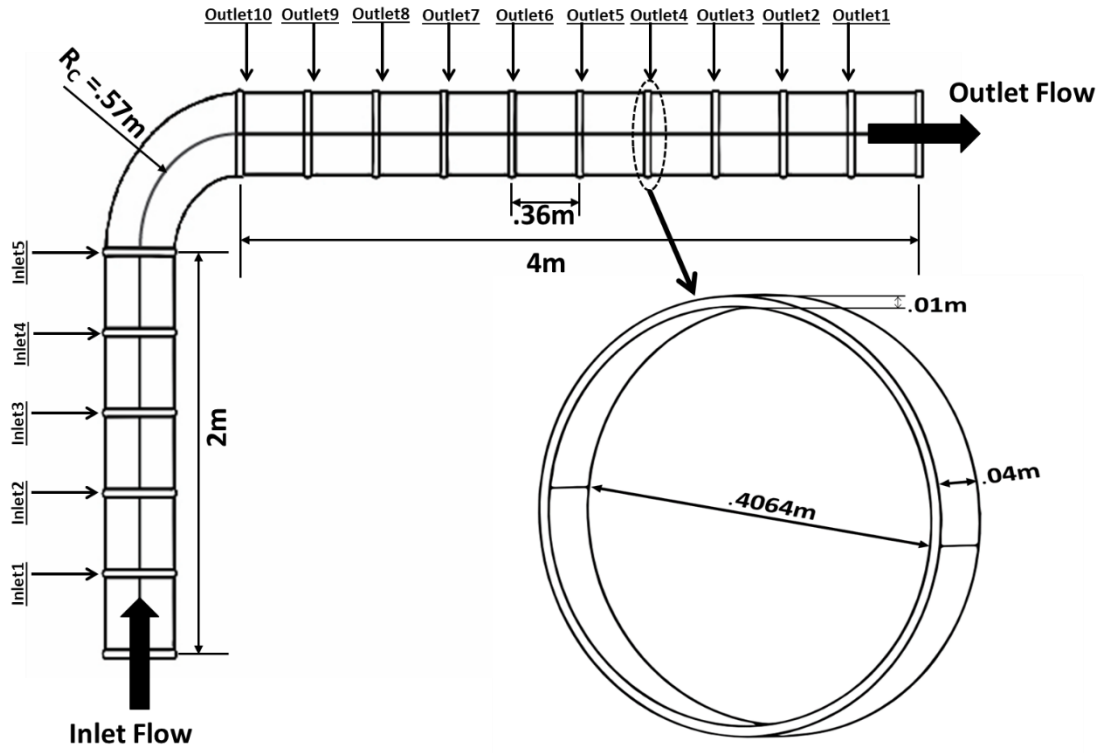

Figure 2: Pipe and clamp structure geometry

In this study, 15 potential clamping positions along the pipe are identified, equally spaced for consistency in measurement. These positions are divided into two segments: five positions in the upstream length, labelled as Inlet1 through Inlet5, and ten positions in the downstream length, labelled as Outlet1 through Outlet10. Each clamp is positioned with a 36 cm gap to ensure uniform distribution. These clamps are a simplified representation of actual clamps, designed with a width of 4 cm and a thickness of 1 cm and constructed from stainless steel, as shown in **Table 2**. Combining one or more clamping positions and numbers is used for each of the vibrational analyses. The rest of the clamps are suppressed during the simulation. After simulating all the possible combinations of the clamping position, the optimum position of the clamp is determined where the vibration and deformation of the pipe are minimised.

Table 1: Pipeline Specifications

Pipe Schedule	Material	Outer Diameter (m)	Elbow radius (m)	Wall Thickness (m)
SCH100	Carbon Steel	0.4064	.570	.02619

Table 2: Clamp Specifications

Clamp Material	Clamp Inner Diameter (m)	Thickness (m)	Width
Stainless Steel	0.4064	.01	.04

For further analysis, the structural domain is discretized into more minor elements. A sensitivity analysis was performed to determine the optimal number of elements so that the

results converge and the computational time can be minimized. Two probable clamping was done to get a comprehensive idea of the element numbers, one at the upstream and one at the downstream length. **Figure 3** compares maximum accelerations (in m/s²) and simulation time (in minutes) against the number of elements. The horizontal axis represents the number of elements, ranging from 6000 to 14000. The vertical left axis measures the maximum acceleration, plotted in red, which shows that as the number of elements increases, the max acceleration decreases and converges when the element number is 9600. The elbow and the clamps are meshed as finely as possible, as these are the most critical computational areas.

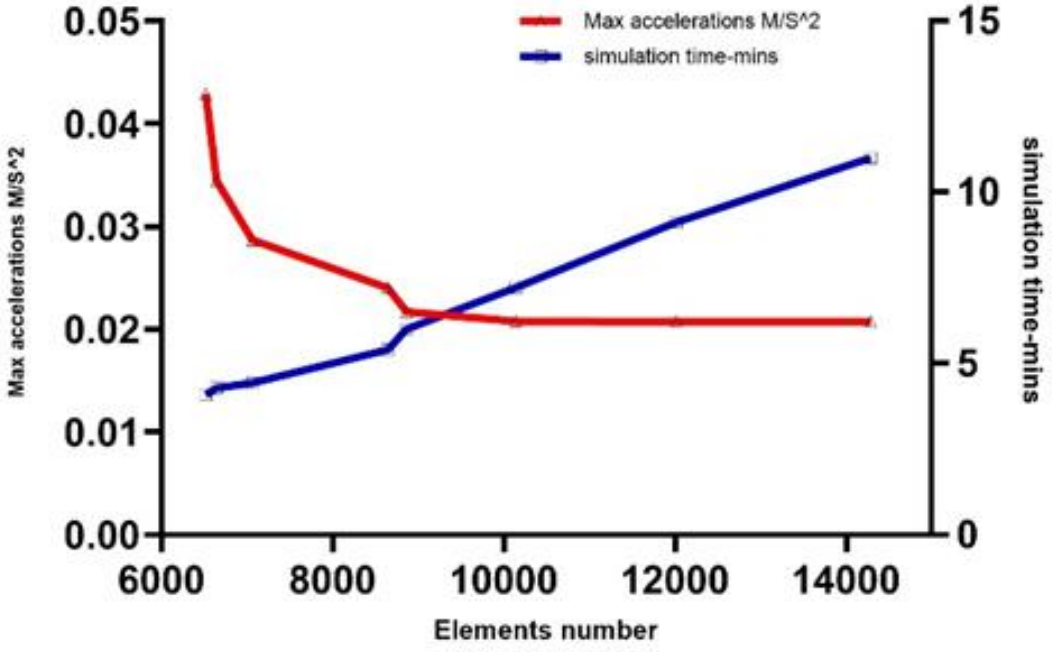

Figure 3: Sensitivity Analysis

To set the boundary condition, as shown in **Figure 4**, the downstream portion of the pipe is regarded as being connected to an extended section of the pipe. Consequently, the movement of the outlet is restricted to the transverse direction, allowing the movement only in the axial direction.

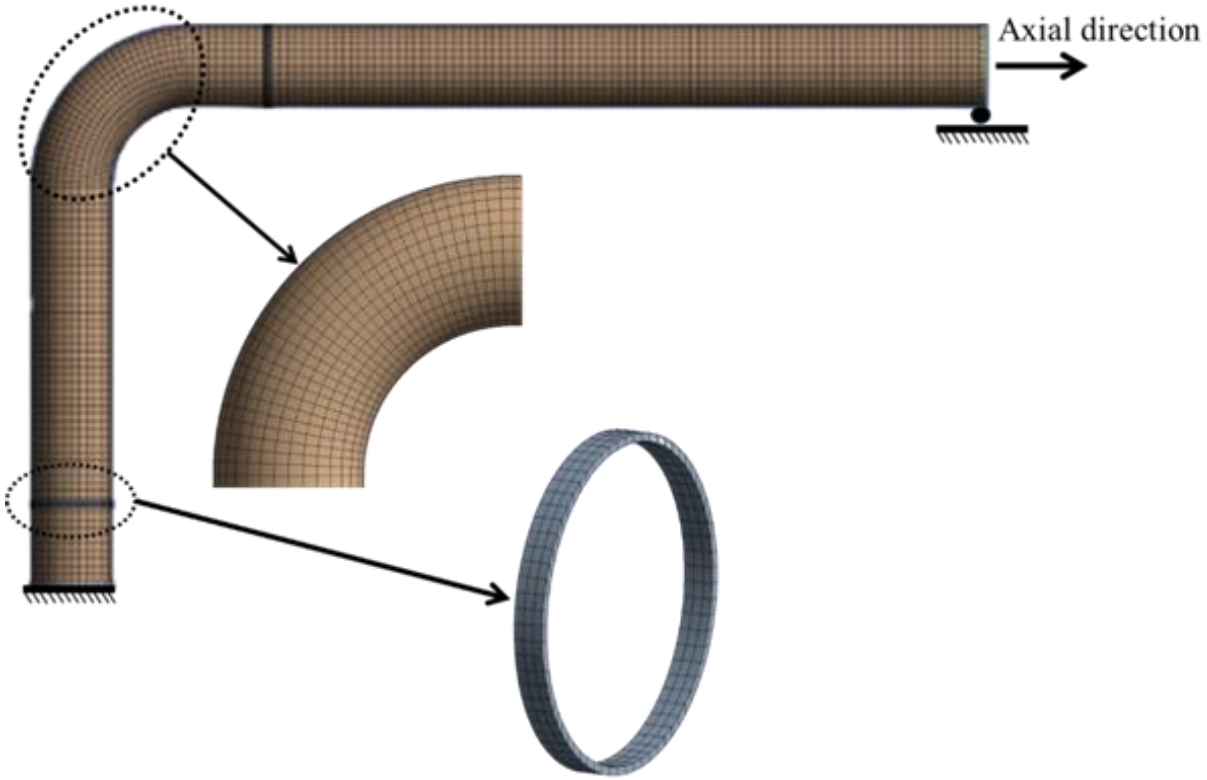

Figure 4: Mesh and Boundary condition of structural domain

The pipe is directly connected to the boiler outlet at the inlet, establishing a real-world scenario where the inlet portion is completely fixed. Additionally, the interaction between the clamp and the pipe is assumed to be frictionless under an ideal case scenario. This simplification is intended to eradicate the effect of the damping force itself, eliminating the influence of friction between the pipe and the clamp. The outer surface of the clamp is considered to be fully fixed.

3.2 Fluid Domain:

The fluid used in this system is steam-heated to a high temperature. The distinct characteristics of the superheated steam utilized in this analysis are obtained from the operational data of a boiler system. The characteristics are shown in **Table 3**.

Table 3: Fluid Properties

Pressure (MPa)	Density(kg/m^3)	Viscosity (μPa.s)	Mass Flow Rate (Kg/s)		
			1	2	3
12.58	36.594	29	180	200	220

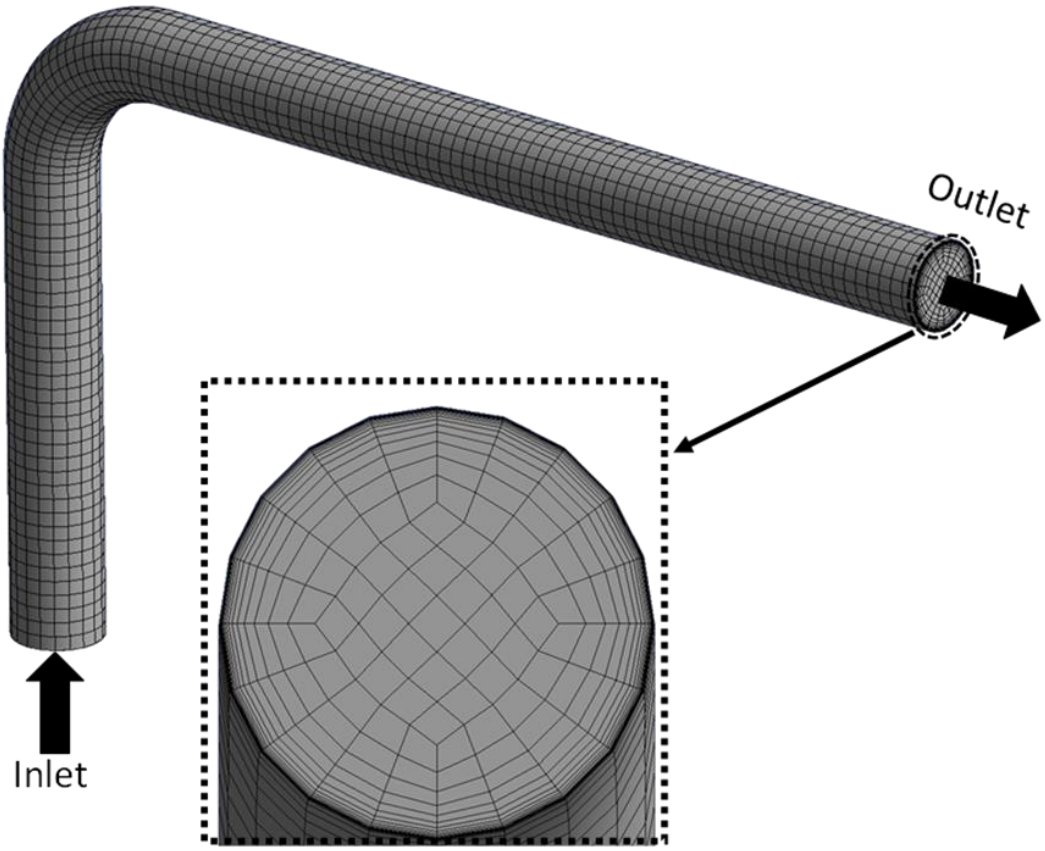

Figure 5: Mesh for fluid domain

The fluid domain was meshed with a few parameters in consideration. During the simulation, the y^+ value had to be small enough to cover the viscous sublayers (approximately 5) [26]. This is an essential consideration as the layers around the bent region of the pipe have complex geometry and need a smooth element distribution to capture the data accurately. The wall y^+ was kept at a steady 1.15 throughout the simulation to capture the data at the wall sublayers. Properly structured mesh was also necessary to get consistent data across the inner and outer layers of the fluid domain. An O-grid type mesh was selected with hex-dominant elements as it gives a structured formation for the mesh elements throughout the fluid domain, as shown in **Figure 5**. The aspect ratio was maintained at 1.29, with a mesh element number of 60,256. This ensured the edges of the mesh elements were mostly similar in length and the simulation time was as low as possible.

As for the boundary condition at the inlet, three different mass flow rates are used: 180 kg/s, 200 kg/s, and 220 kg/s [27]. The outlet pressure is kept as atmospheric pressure. The operating pressure of the simulation is set to be 12.58 MPa [27]. Static wall, no-slip condition was set. Reynolds stress model with enhanced wall treatment is used as a solver model for the analysis.

3.3 Simulation Setup:

ANSYS-Workbench is used to integrate different simulation modules for a comprehensive analysis. The setup is shown in **Figure 6**.

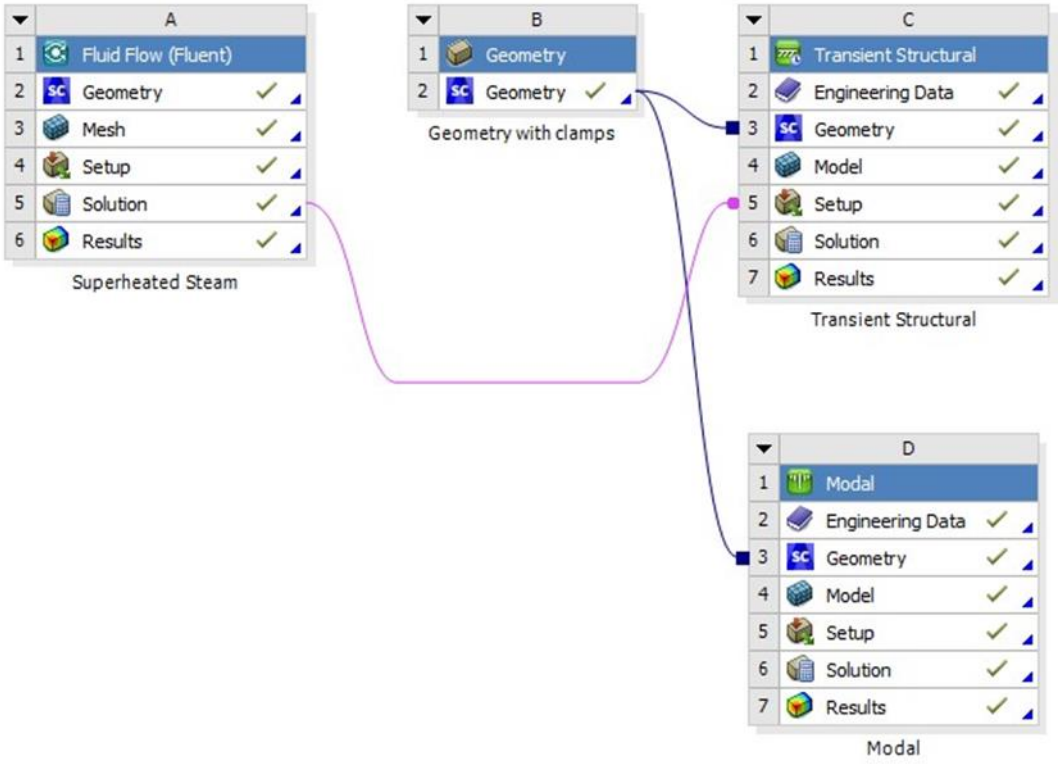

Figure 6: Simulation Setup

Fluid Flow (Fluent): The Ansys fluent module simulates the fluid dynamics within the pipe. In this module, the simulation procedure starts by creating the fluid domain geometry. Then, the geometry is meshed into more minor elements to capture the complex flow characteristics within the pipe. The procedure is continued by configuring the simulation parameters, such as the fluid's boundary conditions and physical properties. After this, the solver is executed using the proper solver model, and the Reynolds stress model is used in this case. The results from this module show the fluid behavior throughout the pipe, which is critical for further structural analysis.

Transient Structural: This module assesses how the pipe structure and clamps respond to the dynamic loads and stresses the moving fluid induces. The setup includes configuring the material, discretizing the domain, and boundary conditions. The pressure distribution from the Fluid Flow (Fluent) module is imported into the transient structure module to map the load throughout the pipe's inner wall. The resulting data shows how the fluid affects the structural domain regarding acceleration, deformation, etc.

Modal Analysis: The modal analysis module is used to determine the natural frequency of the structural domain, which is essential in understanding the vibrational characteristics of the system. It helps to understand the resonant frequency, which leads to failure in the system due to fatigue or excessive vibration.

Chapter 4: Model Validation

The validation process involves comparing the simulation results with those from a previously established study by Abuhatira. This process includes validating the fluid configuration, and then the structural configuration is validated. As Abuhatira's work is validated with experimental work, thus this comparison helped us confirm that our model accurately represents the physical phenomena.

In his paper, Abuhatira's primary objective was to improve the accuracy of leakage detection in a pipeline system using the vibrational effects caused by the leakage. To determine the effects of the leakage due to fluid flow through the pipeline, his study focused on modelling the interactions of fluid dynamics and structural mechanics within the pipeline. All the necessary data for his study are collected from Mellitah Oil and Gas Company, Libya, which include fluid properties, i.e., fluid density, Reynolds number, kinematic viscosity, and structural properties, i.e., pipe material specification, boundary condition and elbow features.

In Abuhatiras's work, he used crude oil as a working fluid. The properties of the fluid are given in **Table 4.**

Table 4: Fluid Properties of Abuhatira's Study[42]

Pressure (Mpa)	Density(kg/m^3)	Viscosity (Pa.s)	Velocity (m/s)
4	694	0.00122	0.5

As pressure and velocity are the main components in the fluid domain, in his study, he showed how pressure and velocity contour are distributed throughout the pipeline.

Figure 7 shows the velocity and pressure contour from Abuhatura's study when crude oil flows through the bend. In his study, as shown in **Figure 7a**, the velocity increases in the inner pipe of the wall near the inlet and decreases at the outer pipe wall. He showed how pressure distribution causes a secondary flow due to an imbalance between pressure gradient and centrifugal force, as the highest pressure is concentrated in the canter elbow at the outer radius of the pipe, as shown in the **Figure 7b**. This procedure is followed for both with leak condition and without leak condition. As pressure is the main component that causes the vibration, he compared the pressure contour for both with leak and without leak conditions, as flow field data differs from without leak condition to leak condition.

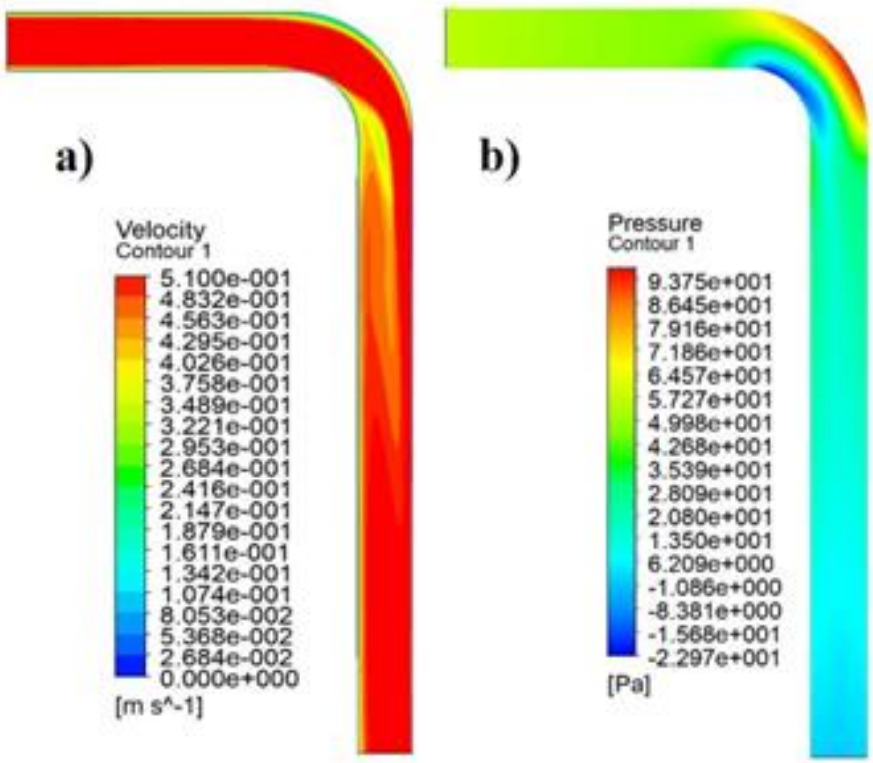

Figure 7: Velocity and Pressure Contour of the 90-degree Pipe Elbow of Abuhatira's Study

This pressure data then imported into the structural domain, where there are 6 configuration is applied

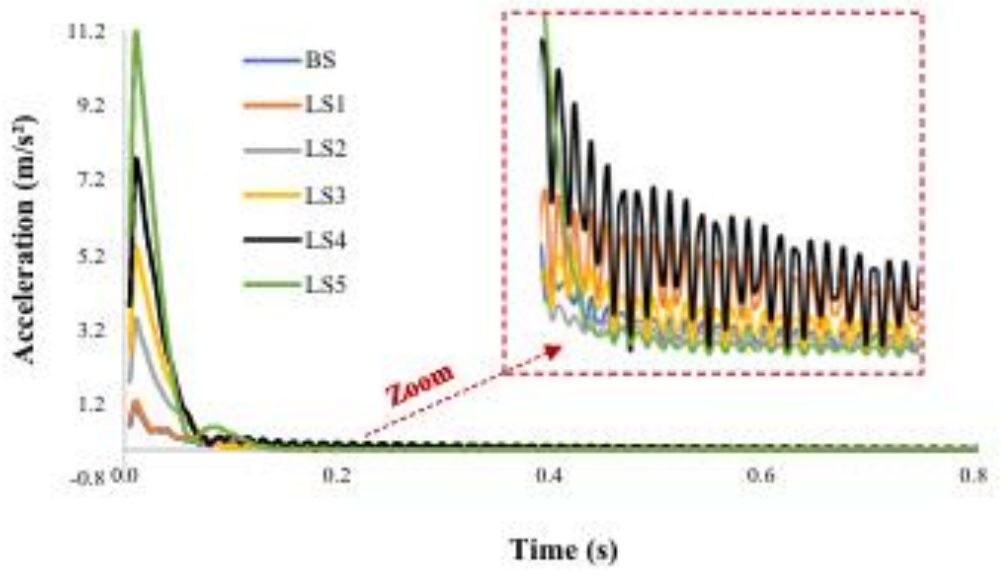

Figure 8: Vibration signals in the time domain for all cases[42]

Figure 8 shows multiple accelerations vs time curves, each representing a different scenario within the pipeline system

BS: Baseline System (BS) represents the pipeline acceleration response under normal conditions when no leak is present. This is a reference line for those with a leak in the pipeline system.

LS: Leak Sensitivity Lines are lines corresponding to different leak conditions. Each LS line consists of leaks of different sizes and shapes. These lines are labelled from LS1 to LS5, where LS1 represents the smallest leak, and LS5 represents the largest leak.
The graph shows a clear variation in acceleration amplitude across all the conditions. The normal conditions show relatively low amplitude compared to the leaking conditions. This deviation of LS lines from the BS lines indicates the presence of the leaks.

4.1 Fluid Model Validation:

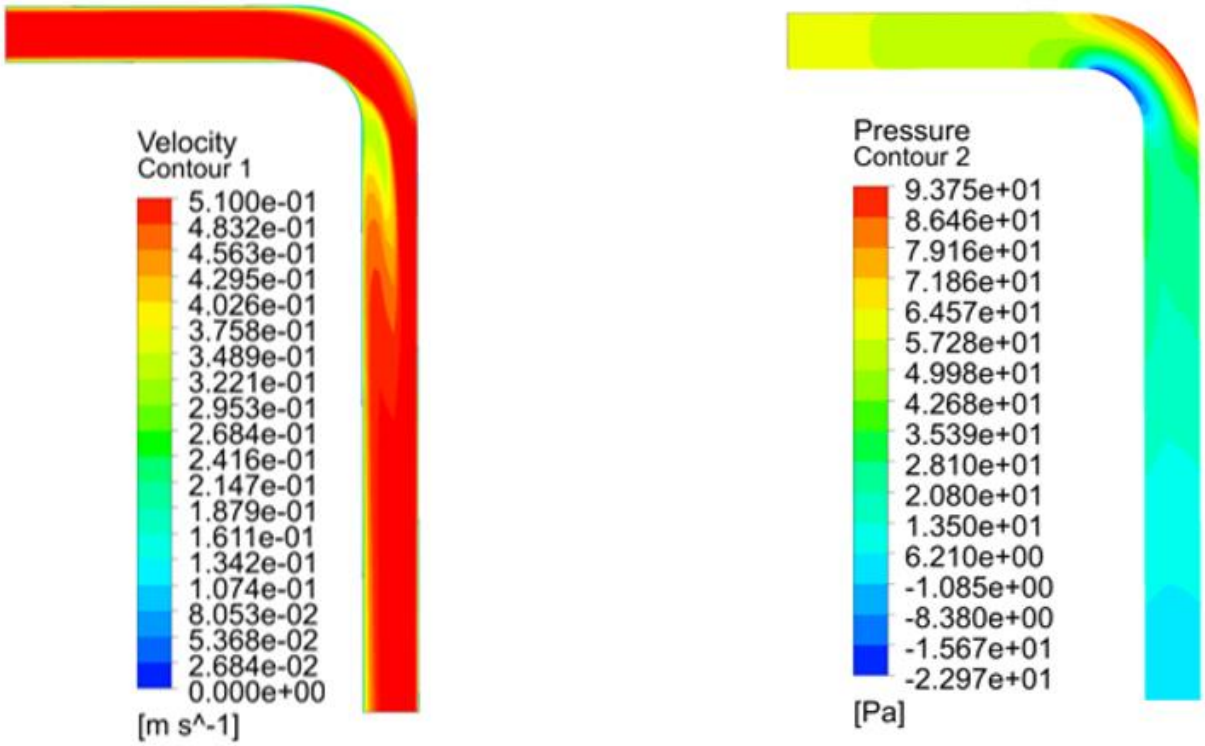

Figure 9: 9a) Velocity Contour
9b) pressure Contour (Crude Oil)

Here, **Figure 9a** shows the velocity contour from Ansys Fluent. The contour indicates the velocity distribution along the pipe due to the flow of crude oil inside the pipe. Comparing this velocity distribution with **Figure 7a** shows a similar pattern in the flow and magnitude.
On the other hand, **Figure 9b** shows the pressure contour from this study using crude oil as fluent. Comparing this data with Abuhatira's work [21], as shown in **Figure 7b**, which depicts similar pressure distribution patterns and magnitude. The magnitude of the pressure throughout the pipe ranges from approximately 93.75 Pa to -22.97 Pa, which closely matches the simulation results.

4.2 Structural Model Validation:

The structural configuration is validated by comparing the acceleration of the structure extracted from the transient structural results with the baseline acceleration of Abuhatira's work.

Figure 8 shows the acceleration of the structural domain over time. In the study, Abuhatira showed acceleration for six different cases [21]. Where LS1 to LS5 shows acceleration when there is a leakage in the piping system, the BS line shows the baseline configuration where there is no leakage. We have compared the simulation results with the BS line acceleration data, as shown in **Figure 8**, to validate our structural configuration.

Figure 10 shows the acceleration vs time graph, which shows the impact of the pressure extracted from the fluid domain used. The boundary condition and domain geometry are the same as those in the study of Abuhatira. There is an initial spike in acceleration followed by a rapid drop, which shows the dynamic behavior of the structural domain. The maximum acceleration is approximately 1.5 m/s^2.

As we compare the acceleration data from **Figure 10** with the BS line acceleration data from **Figure 8**, a similar trend and magnitude can be seen, which validates the structural configuration in this study.

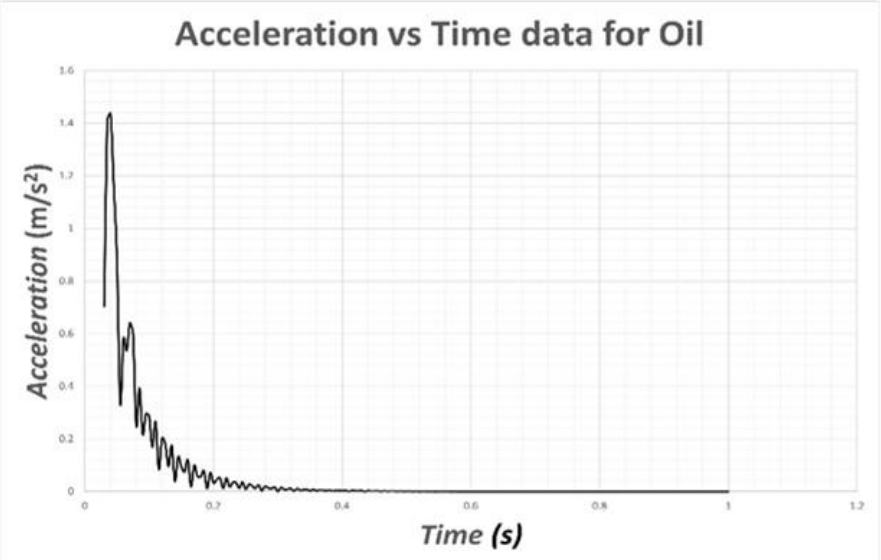

Figure 10: Structural setup validation for oil flow through bent pipe

5. Computational Analysis

The vibration response of the pipe elbow segment is simulated using the FSI model of the current study by coupling the RSM solving the viscous sublayer with the transient structural FEA analysis. The frequency response was analyzed through FFT to determine the amplitudes for the varying mass flow rates.

Simulations for varying flow rates were performed instead of one static flow rate because the real-world scenario showcases mass flow rates that are not static[43]. An analysis was done to determine the unclamped frequency magnitude. Clamping was done at strategic locations along the pipe segment to minimize deformation and acceleration magnitudes. The optimum number and location of clamps were determined based on the reduction of amplitudes for both acceleration and deformation.

Table 5: Distributions of pressure and velocity for varying flow rates

Mass flow rate	**180 kg/s**	**200 kg/s**	**220 kg/s**
Maximum pressure (Pa)	18731.38	23075.97	27870
Maximum velocity (m/s)	59.88	66.56	73.23

Due to the use of high-velocity superheated pressurized steam, the vortex was generated around the elbow location. This creates a pressure difference along the outer and inner radius of the elbow compared to its surrounding areas, creating vortex-induced vibration. The pressure distributions for the different mass flow rates are shown in **Figures 11a, 11b, and 11c** for the mass flow rates of 180 kg/s, 200 kg/s, and 220 kg/s respectively. Due to the nature of the fluid, the vibration signals have a large amplitude. It was noticed that higher mass flow rate values

Table 6: Modes

Modes	**Frequency (Hz)**
1st	24.465
2nd	35.043
3rd	66.328
4th	88.149
5th	191.12
6th	192.77

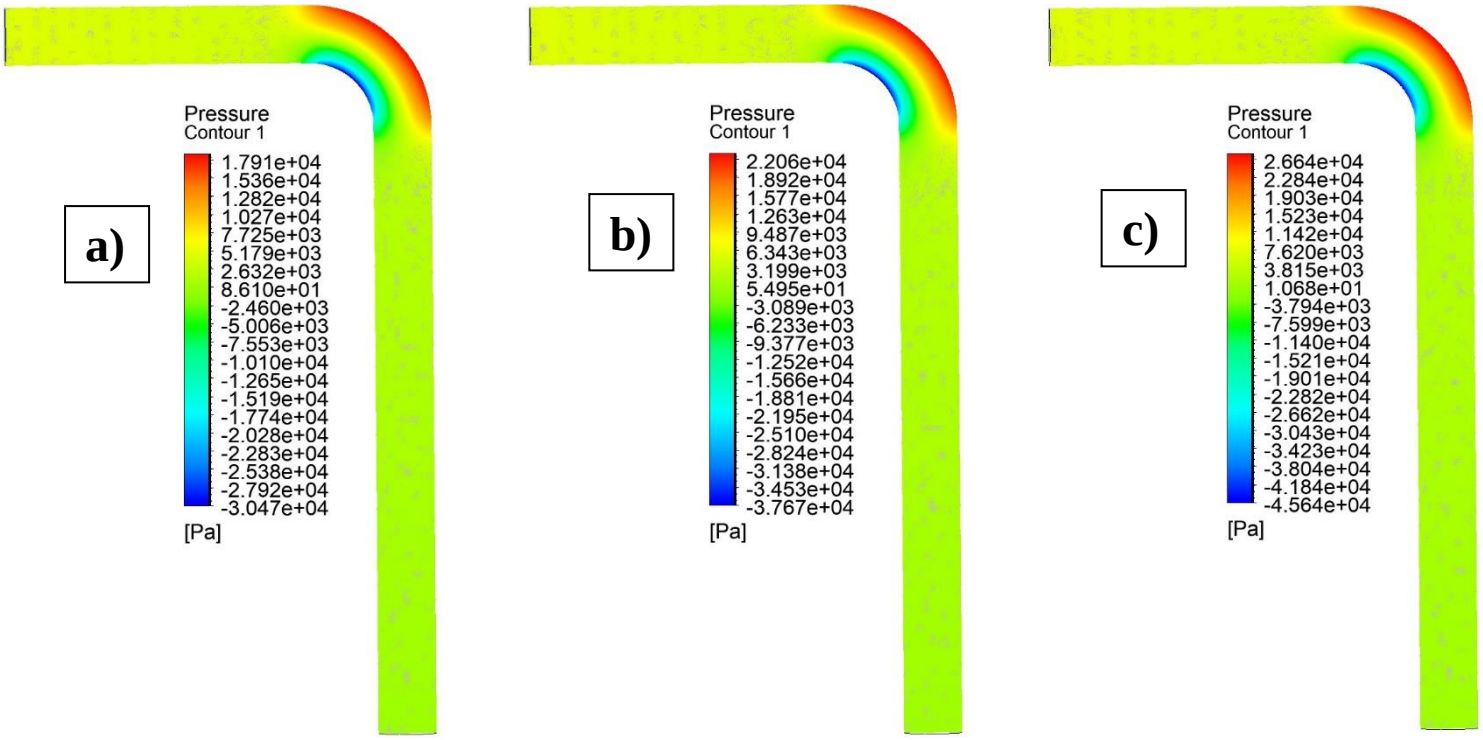

Figure 11: Pressure Contour a)180kg/s, b)200 kg/s, c)220 kg/s

resulted in higher maximum pressure, which is denoted in **Table 5**, and thus higher amplitude values for both acceleration and deformation of the pipe segment.

The acceleration and deformation signals were transformed from the time domain to the frequency domain using the Fast Fourier Transform (FFT). FFT allows the signal to be converted into individual spectral components which is important to find the resonance peaks from the acceleration and deformation data. The clamps were modeled in a simplified manner to reduce simulation time. A total of 15 clamp locations have been tested across various positions throughout the pipe segment. The locations are shown in **Figure 2**. The optimal positions were determined based on the amplitude reduction amount of each clamp individually. The chosen location for the single clamp was fixed and then the rest of the 14 positions were tested again. The optimal number of clamps to be used was explored following this.

5.1 Modal Analysis

Modal analysis was performed to understand the modes and natural frequencies of the unloaded and unclamped pipe segment. The first 6 modes were considered during the analysis. This analysis served as a comparison point for the frequency domain amplitudes. A high amplitude on any of the modes may require further clamping to avoid in case of certain flow rates. The total deformation plots for each of the modes are shown from **Figure 12 to Figure 14**. Each of the modes and their respective frequencies are shown in **Table 6**

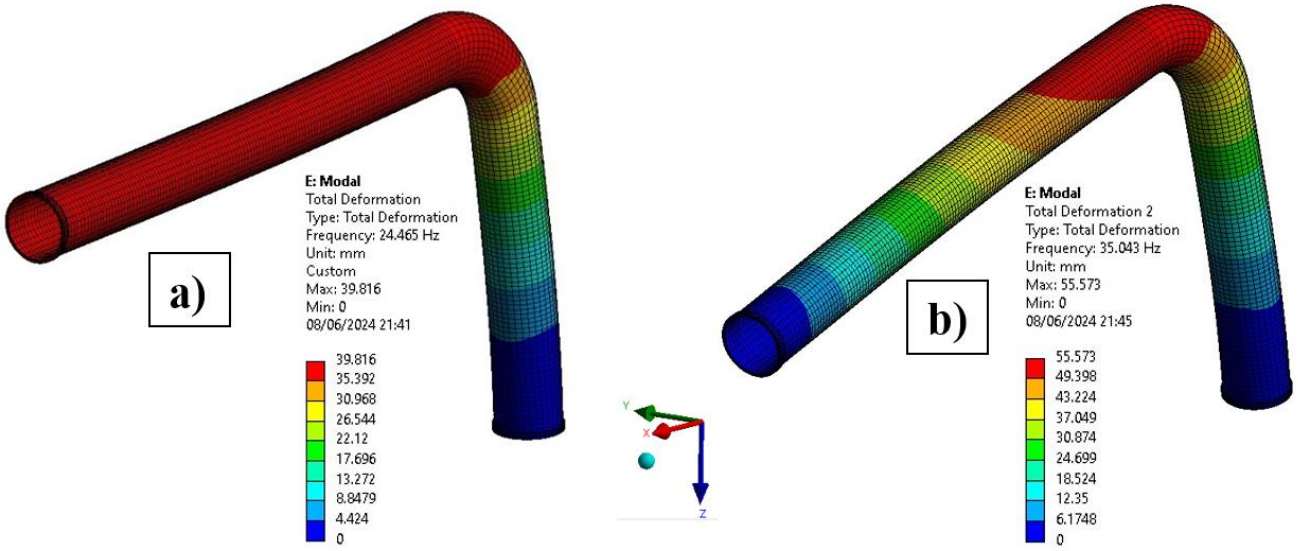

Figure 12: Modes a)1st, b)2nd

There are distinct modes that occur at specific frequencies that characterize the deformation of a pipe under vibrational stress. These modes characterize the axial and transverse movement of the pipe as well as the locations of nodes, or places where there is no movement, along its length. It is essential to comprehend these modes to anticipate and address possible problems like resonance, which might result in structural failure. An expanded examination of every mode of deformation is provided below:

First Mode - 24 Hz: Axial Reciprocation In the *X*-Axis
The pipe shows axial reciprocation along the *X*-axis at 24 Hz. This mode moves back and forth the entire length of the pipe. This kind of movement implies that the pipe behaves like a longitudinal wave as it expands and compresses. This mode is important because it frequently matches the system's fundamental frequency, which causes the whole pipe length to move simultaneously and may cause large stress concentrations at specific spots.

Second Mode – 35 Hz: Reciprocation Along the *Y*-Axis

The second mode, which has reciprocation along the *Y*-axis, happens at 35 Hz. Lateral movement perpendicular to the pipe's length occurs in this phase. The pipe is swaying from side to side, indicating a bending vibration. This lateral movement can cause fatigue and eventual failure at the sites of connection; therefore, it can be especially problematic if the pipe is subject to attachments or constraints that limit its movement.

Third Mode - 66 Hz: Node Halfway Downstream with Reciprocation Along the *Z*-Axis

Halfway down its length, the pipe exhibits reciprocation along the *Z*-axis at 66 Hz, forming a node. One segment of the pipe moving out of phase with the other is indicative of a transverse wave in this mode. When a node is present, the pipe is divided into two vibrating segments by a point that is stationary along its length. Significant bending stress may result from this mode, particularly at the node and antinode locations which are the points of highest displacement.

Fourth Mode - 88 Hz: Two Nodes with Reciprocation Along the *Y*-Axis

The fourth mode, which happens at 88 Hz, has two nodes along the body of the pipe and reciprocation along the *Y*-axis. With three vibrating segments in the pipe, this mode is more intricate. Sections between the extra nodes move out of phase, signifying places where there is no movement. This mode necessitates careful consideration in design and support placement because it can lead to complex stress distributions and possible areas of failure where the segments join.

Fifth Mode - 191 Hz: Two Nodes Downstream with Reciprocation Along the *Z*-Axis.

The fifth mode, which involves reciprocation along the *Z*-axis to create two nodes downstream, occurs at 191 Hz. This option splits the pipe into three pieces on a different axis than the fourth mode. The pipe vibrates in sections between the nodes, which represent stationary places. This higher frequency mode, especially in areas with fast movement changes, suggests a more complex vibrational pattern that may cause problems with high-frequency tiredness.

Sixth Mode - 192 Hz: Two Nodes Downstream with Reciprocation Along the *Y*-Axis.

The sixth mode, which has two nodes downstream and reciprocates down the *Y*-axis, occurs at 192 Hz. Though it occurs on a different axis and at a little higher frequency than the fifth mode, these two modes are extremely similar. Again, the presence of two nodes results in three vibrating segments, indicating the existence of a highly complex and dynamic vibrational state. Due to its proximity to the fifth mode, which may cause resonance if the frequencies coincide, this mode can be very difficult to control.

It is clear from **Figures 12 through 14** that these modes exhibit total deformation variations ranging from 40 mm to 72 mm. The range of deformation shows that the pipe moves significantly, which needs to be taken into account while designing and maintaining the piping system. The various reciprocation modes shed light on potential motions that might occur during resonance at related frequencies. Comprehending these modes helps in predicting areas of high stress and possible failure.

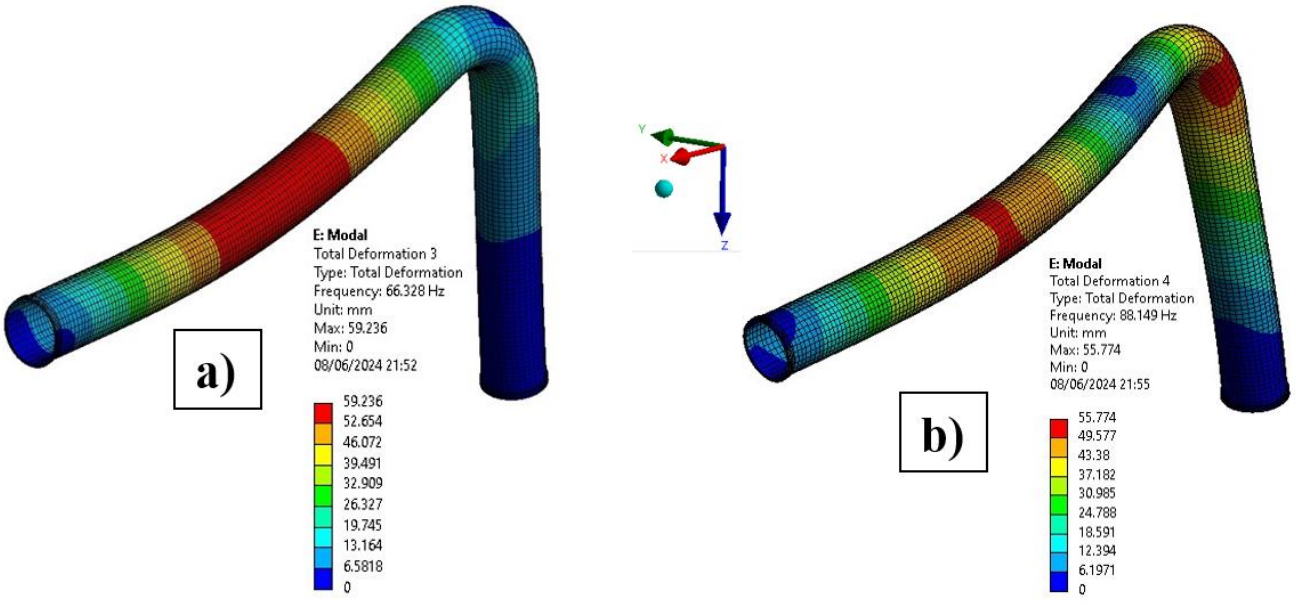

Figure 13:Modes a)3rd, b)4th

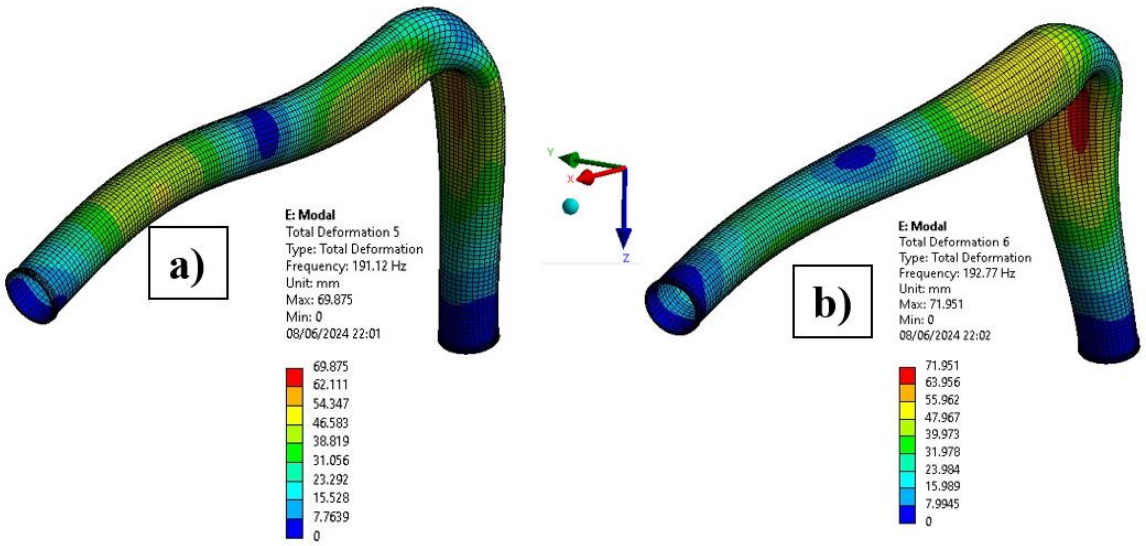

Figure 14: Modes a)5th, b)6th

6. Results and Discussion

The results of the vibration analysis and clamp location optimization are discussed in this section. The results for unclamped and clamped conditions are shown along with the amplitude reduction for acceleration in all the flow rates analyzed.

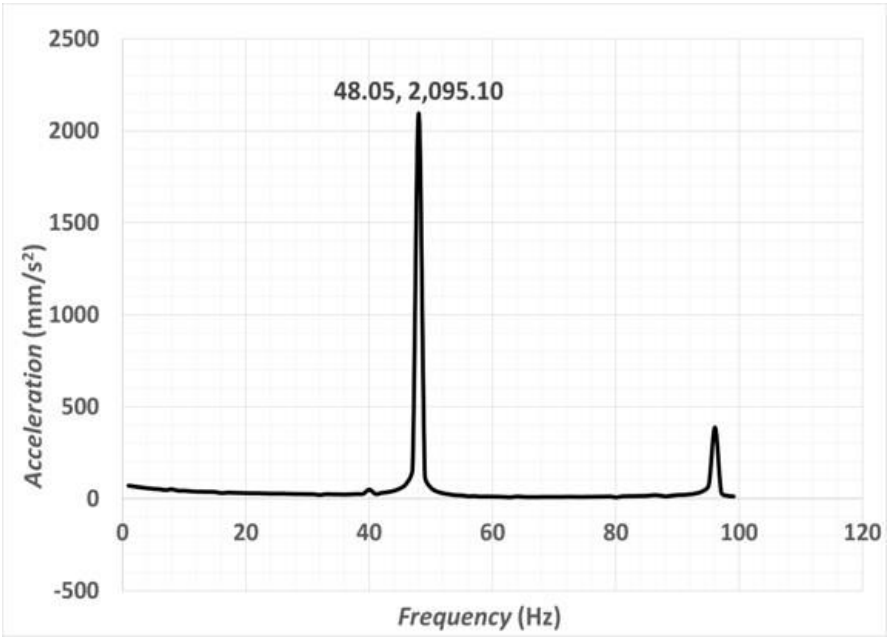

Figure 15: FFT of acceleration for unclamped condition (180 kg/s)

The analysis of the clamp locations was preceded by the analysis of the pipe in unclamped condition with a mass flow rate of 180 kg/s. The highest amplitude of the acceleration data in this case was 2095.10 mm/s^2, at 48.05 Hz. This is shown in **Figure 15** with the acceleration in the *y*-axis and frequency in the *x*-axis.

Each of the upstream positions leading to the bend was analyzed for the mass flow rate of 180 kg/s. These positions have been marked in **Figure 2**. Here, a variation in the frequency of the highest amplitudes of acceleration for each location was observed. This is due to the flow not being fully developed[44]. The inlet of the pipe was considered to be directly connected to the boiler. This is why the flow is considered to be underdeveloped. The position of INLET1 showed the resonance at the nearest frequency of the unclamped condition. This is why it was chosen for further analysis.

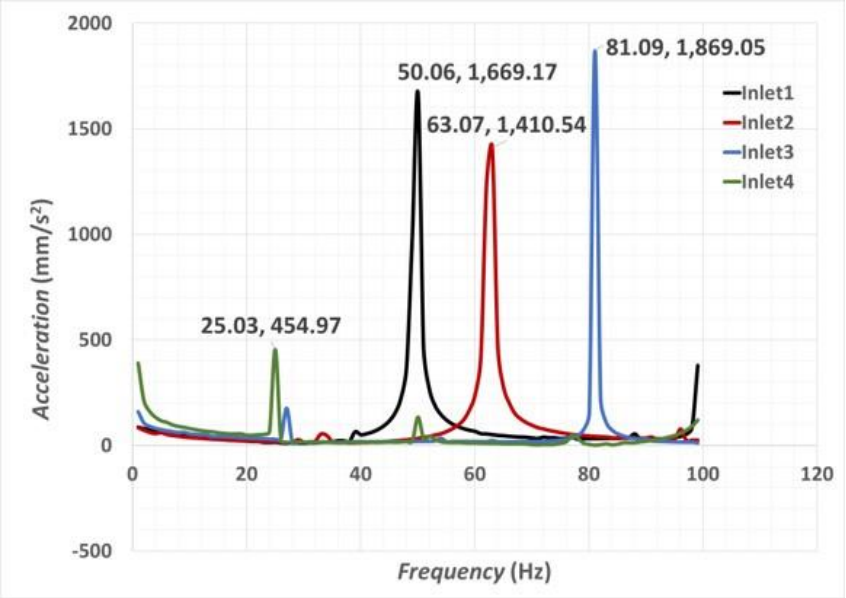

Figure 17:FFT of acceleration for upstream clamp positions (180kg/s)

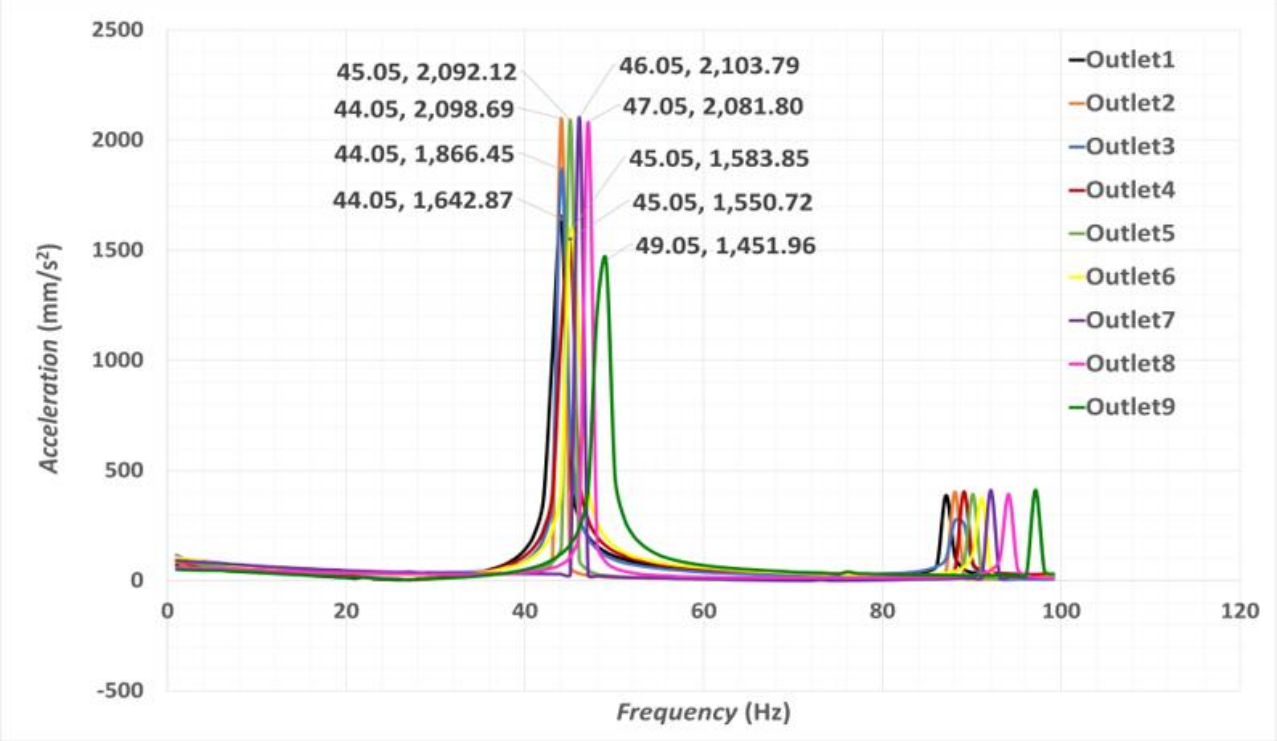

Figure 16:FFT of acceleration for downstream clamp positions (180kg/s)

A similar analysis showed no variation in the resonant frequency in the case of downstream flow after the bend. The positions have again been shown in **Figure 2**. However, the lowest amplitude of acceleration was found to be for the location of OUTLET9. This was considered for further analysis.

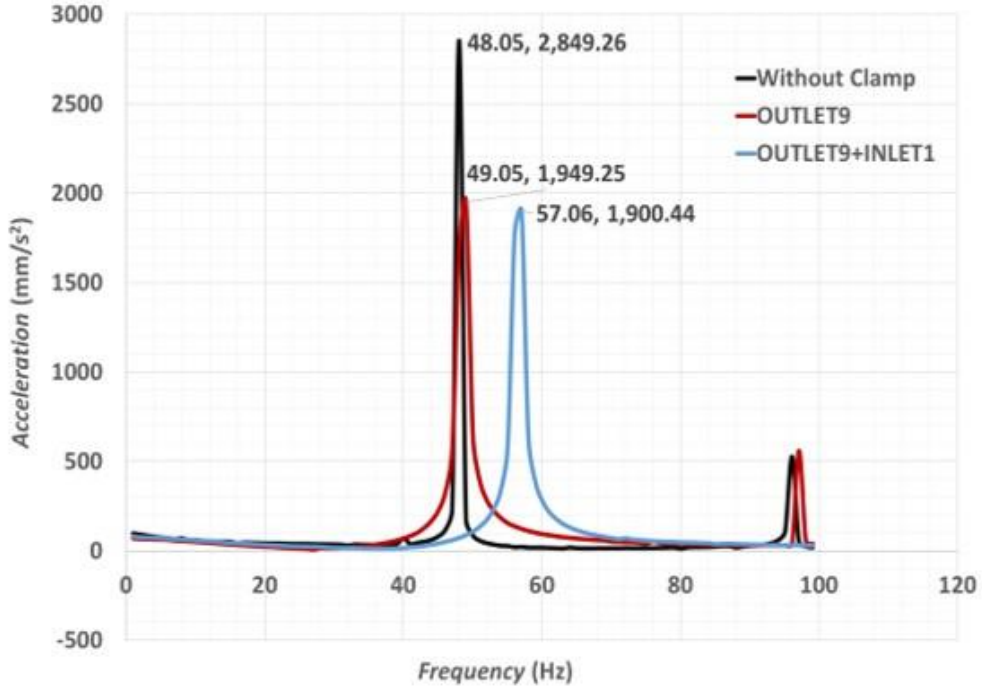

Figure 19:FFT of acceleration for 180 kg/s flow rate

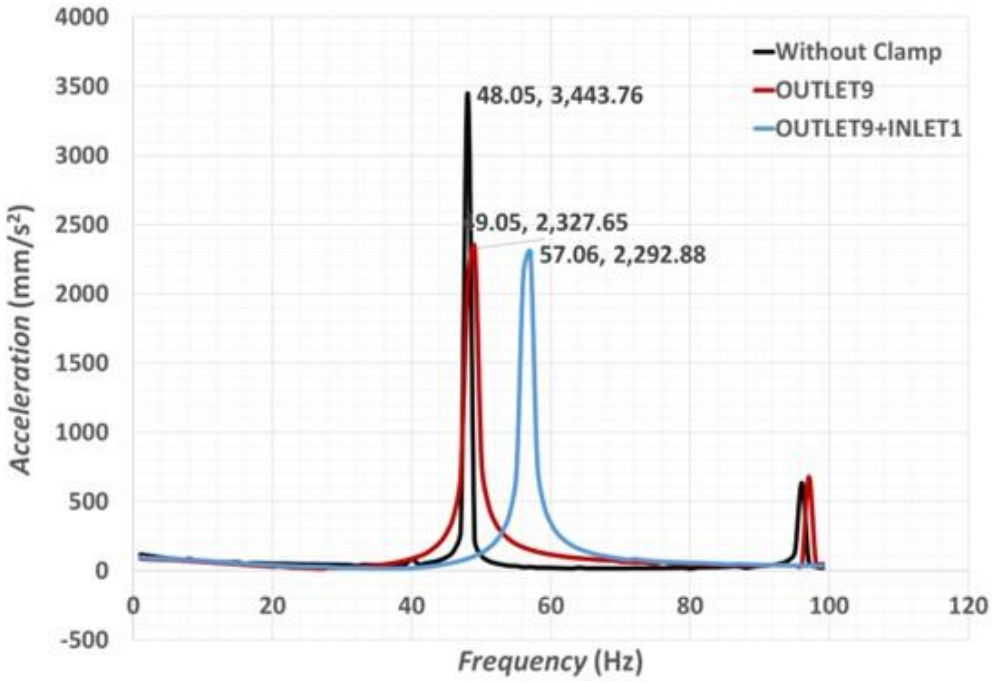

Figure 18:FFT of acceleration for 200 kg/s flow rate

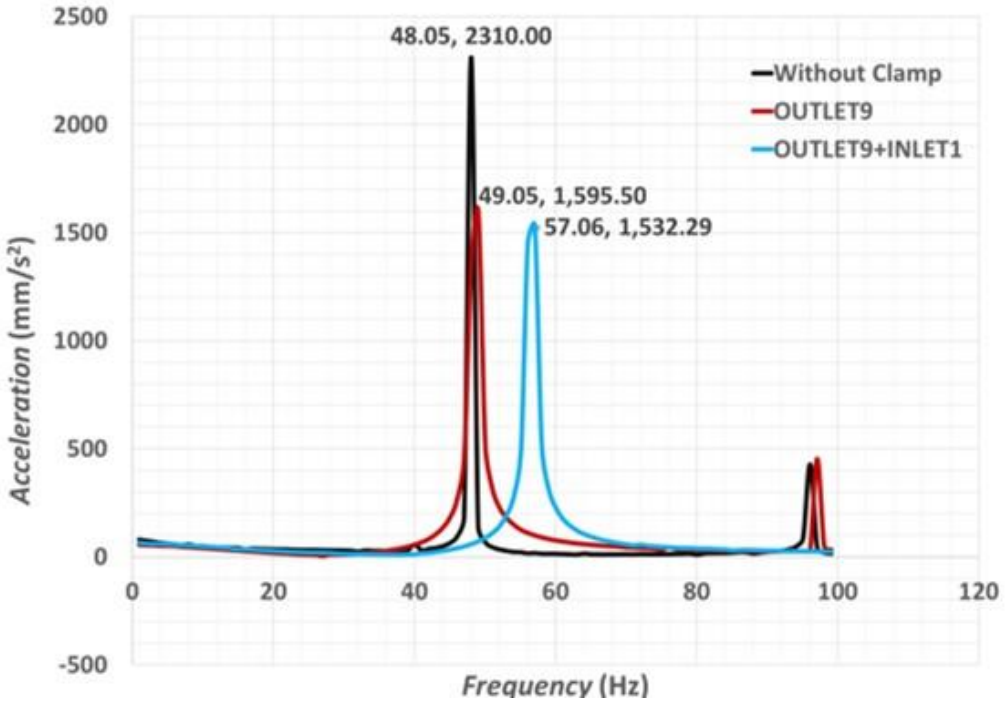

Figure 20:FFT of acceleration for 220 kg/s flow rate

Following the analysis of the vibration signals in the frequency domain, it can be seen that clamping at the location of Outlet9 reduces the amplitude of vibration by 30.93%, 31.59%, and 31% for the flow rates of 180 kg/s, 200kg/s, and 220 kg/s respectively. However, adding an additional clamp at location Inlet1 will reduce 33.67%, 33.30%, and 33.42% for the flow rates of 180 kg/s, 200kg/s, and 220 kg/s respectively. The addition of a secondary clamp does not reduce the amplitude as much. This trend is continued forward with diminishing returns following each addition of a clamp. This trend of diminishing returns is visible from **Figures 18, 19, and 20** which showcase the amplitudes for each clamping condition analyzed in the frequency domain. The amplitudes and reduction rates of each clamping condition for the different mass flow rates are summarized in **Table 7**

Table 7: Acceleration results for different mass flow rates

	Amplitude (mm/s^2) in the Frequency Domain for different clamping setup			**Reduction (Percentage)**	
Mass Flow rate	Unclamped	Clamp at OUTLET9	Clamp at OUTLET9+INLET1	Clamp at OUTLET9	Clamp at OUTLET9+INLET1
180 kg/s	2310	1595.50	1532.29	30.93%	33.67%
200 kg/s	2849.26	1949.25	1900.44	31.59%	33.30%
220 kg/s	3443.76	2327.65	2292.88	31%	33.42%

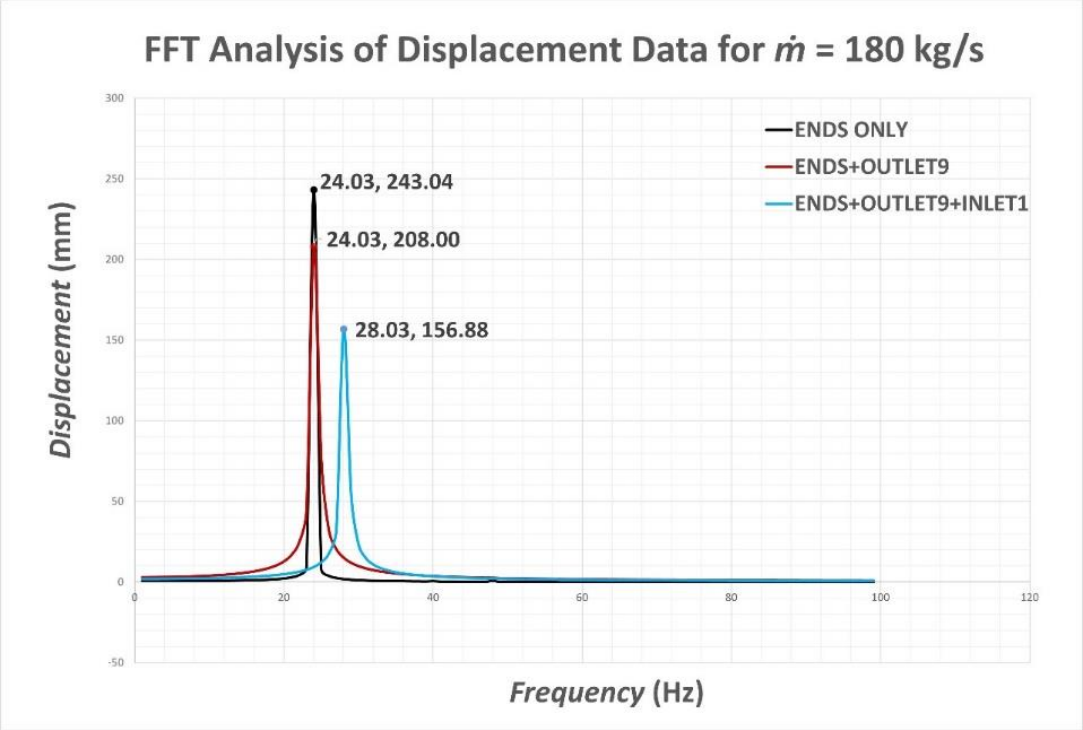

Figure 21: FFT of displacement data for 180 kg/s flow rate

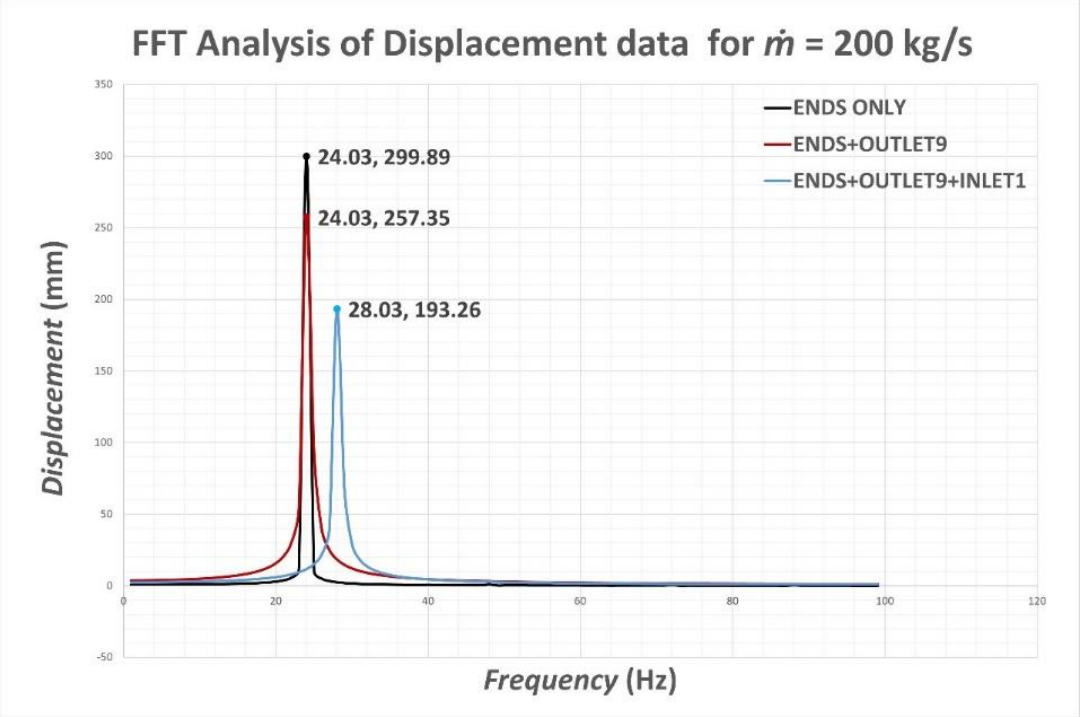

Figure 22:FFT of displacement data for 200 kg/s flow rate

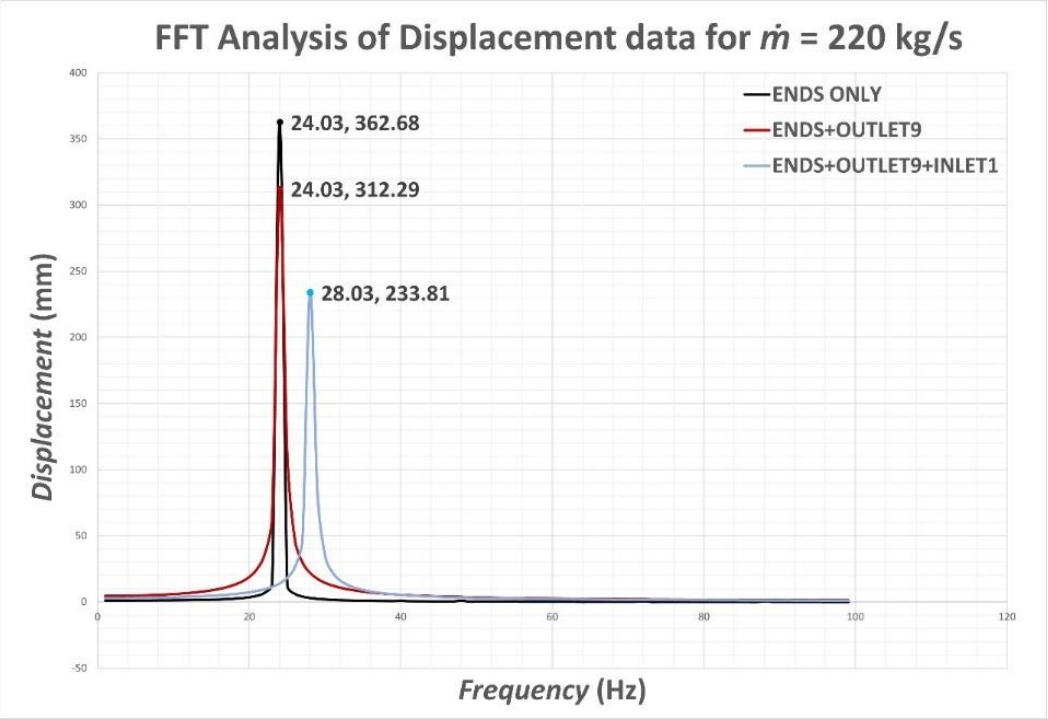

Figure 23: FFT of displacement data for 220 kg/s flow rate

Following the analysis of the deformation data in the frequency domain, it can be seen that clamping at the location of Outlet9 reduces the amplitude of deformation by 14.42%, 14.19%, and 14% for the flow rates of 180 kg/s, 200kg/s, and 220 kg/s respectively. However, adding an additional clamp at location Inlet1 reduces 35.57%, 35.56%, and 35.52% for the flow rates of 180 kg/s, 200kg/s, and 220 kg/s respectively. Adding a secondary clamp reduced the deformation noticeably, which is visible in **Figures 21, 22, and 23**. These showcase the amplitudes (depicted in the *y*-axis) for each clamping condition analyzed in the frequency domain where the frequencies are shown in the *x*-axis. The amplitudes and reduction rate of each clamping condition for the different mass flow rates are summarized in **Table 8**

Table 8: Displacement results for different mass flow rates

	Amplitude (mm) in the Frequency Domain for different clamping setup			**Reduction (Percentage)**	
Mass Flow rate	Unclamped	Clamp at OUTLET9	Clamp at OUTLET9+INLET1	Clamp at OUTLET9	Clamp at OUTLET9+INLET1
180 kg/s	243.04	208	156.58	14.42%	35.57%
200 kg/s	299.89	257.35	193.26	14.19%	35.56%
220 kg/s	362.68	312.29	233.81	14%	35.52%

Here, it is found that the addition of an extra clamp at location INLET1 has reduced the deformation more than the addition of the first clamp. As the acceleration has diminishing

returns, the cost of adding the clamps rises quickly with very little benefit for vibration reduction. This is why the optimal number of clamps was selected to be 2. This provided a good balance between vibration reduction, deformation mitigation, and cost.
Following the analysis, the optimum location for the clamp downstream from the bend is at OUTLET9, which is located 3.640 m away from the outlet towards the location of the elbow. Similarly, the location for the clamp upstream from the bend is at INLET1, which is located 0.40 m away from the inlet towards the location of the elbow. This is depicted in **Figure 24**

A total decrease of 33.667%, 33.3%, and 32.409% in the amplitude of acceleration data and 35.45%, 35.56%, and 35.53% for the deformation data in the frequency domain are observed for the mass flow rates of 180 kg/s, 200 kg/s, and 220 kg/s respectively.

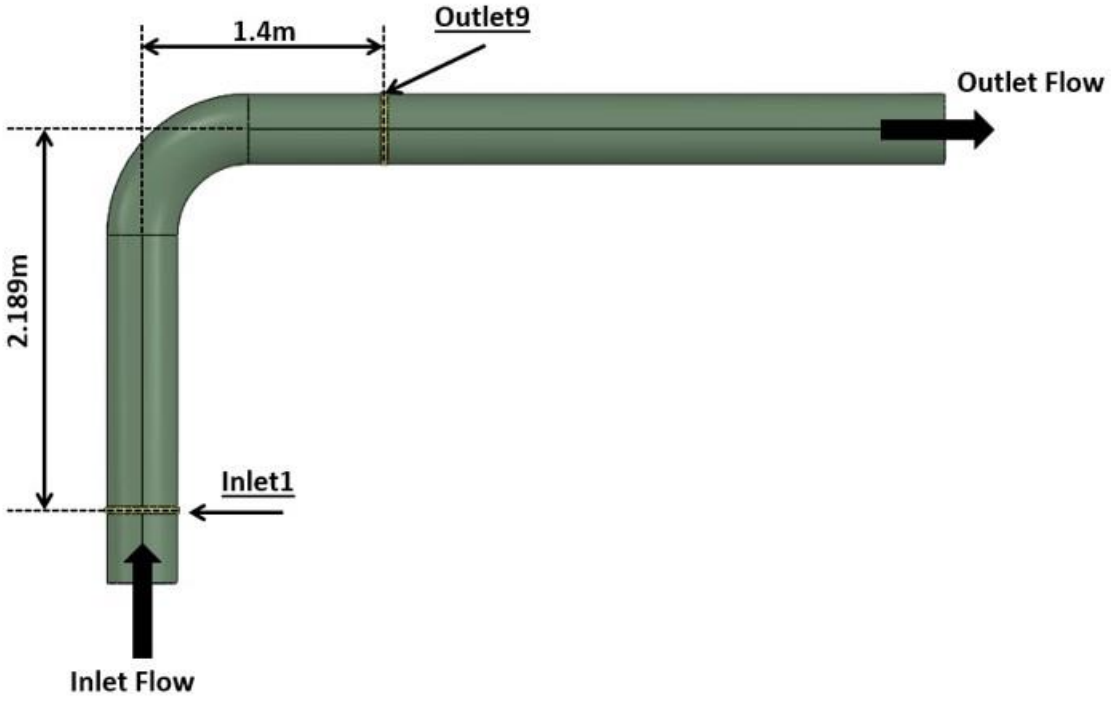

Figure 24:Optimal clamp number and position

7. Conclusion and Future Work

7.1 Conclusion

The main goal of clamp location determination based on vibration analysis for a particular pipe geometry has been achieved through this study. Some key findings are discussed below:

- For the chosen parameters of the pipe, the 1st natural frequency of the pipe is 24Hz. This is the mode where the resonance is observed for the selected boundary conditions. The rest of the modes from 2nd through 6th are observed at frequencies of 35Hz, 66Hz, 88Hz, 191Hz, and 192Hz respectively
- From the FFT of acceleration, using one clamp at the outlet (1.4m from the inlet axis) and another clamp at the inlet (2.189m from the outlet axis) causes the maximum reduction of amplitude of acceleration by 33.67%, 33.30%, and 33.42% for the flow rates of 180 kg/s, 200kg/s, and 220 kg/s respectively.
- From the FFT of displacement, using one clamp at the outlet side (1.4m from the inlet axis) and another clamp at the inlet (2.19m from the outlet axis) causes the maximum reduction of the amplitude of displacement by 35.57%, 35.56%, and 35.52% for the flow rates of 180kg/s, 200kg/s, and 220kg/s respectively.
- The optimal clamp number was chosen to be two as it provided the highest degree of reduction of the displacement amplitude while also not providing diminishing returns for reduction of the acceleration amplitude

7.2 Future Scope

There are however some works that can be done to further build upon this study and investigate the findings in the future. Advancements in this work can be made by following recommendations from the authors:

- Further investigations can be carried out for a range of pipe elbow angles, spanning from 0-180
- Two-way FSI coupling can be used for further accuracy
- Variations of clamp design and materials can be done to investigate pipe elbow vibration
- Optimization of Pipe thickness and clamp thickness for vibration reduction can be done
- Dimensional analysis can be done that incorporates fluid, pipe, and clamp properties

References

[1] Testbook, “Mechanical Vibrations: Definition, Examples, Types, Applications.” Accessed: Jun. 12, 2024. [Online]. Available: https://testbook.com/mechanical-engineering/mechanical-vibrations

[2] Hutchinson engineering, “Engineering Shock & Vibration Definitions - HUTCHINSON.” Accessed: Jun. 12, 2024. [Online]. Available: https://hutchinsonai.com/engineering-capabilities/

[3] “Common Causes Of Piping Vibration And Their Effects On Piping Systems,” TECHNOMAX Middle East Engineering LLC. Accessed: Jun. 12, 2024. [Online]. Available: https://www.technomaxme.com/piping-vibration/

[4] T. Miles, “Piping vibrations | Flow induced & acoustic induced vibrations - DNV,” DNV Oil and gas. Accessed: Jun. 12, 2024. [Online]. Available: https://www.dnv.com/services/piping-vibrations-110735/

[5] J. C. Wachel, J. D. Tison, J. C. " Buddy, and " Wa, “VIBRATIONS IN RECIPROCATING MACHINERY AND PIPING SYSTEMS.”

[6] M. Agar and L. Ancian, “OTC-26784-MS Acoustic-Induced Vibration: A New Methodology for Improved Piping Design Practice,” 2016.

[7] “What is a Vibration Resonance? - Delserro Engineering Solutions.” Accessed: Jun. 12, 2024. [Online]. Available: https://www.desolutions.com/blog/2015/06/what-is-a-vibration-resonance/

[8] “Resonance and Its Effects on Mechanical Structures | Pumps & Systems.” Accessed: Jun. 12, 2024. [Online]. Available: https://www.pumpsandsystems.com/resonance-and-its-effects-mechanical-structures

[9] “Tacoma Narrows Bridge history - Bridge - Lessons from failure,” wsdot . Accessed: Jun. 12, 2024. [Online]. Available: https://wsdot.wa.gov/tnbhistory/bridges-failure.htm

[10] W. Marth, “The Monju accident. Causes and effects,” *Atw. Atomwirtschaft, Atomtechnik*, vol. 41, no. 5, pp. 312–316, 1996, Accessed: Jun. 12, 2024. [Online]. Available: http://inis.iaea.org/Search/search.aspx?orig_q=RN:27060328

[11] “The Broughton Suspension Bridge and the Resonance Disaster | SciHi Blog.” Accessed: Jun. 12, 2024. [Online]. Available: http://scihi.org/broughton-suspension-bridge-resonance-disaster/

[12] “Helicopter Ground Resonance,” Spinning Wings. Accessed: Jun. 12, 2024. [Online]. Available: https://www.spinningwing.com/helicopter/ground-resonance

[13] “Flow-Induced Vibration or FIV in a Piping System with Online Course – What Is Piping.” Accessed: Jun. 12, 2024. [Online]. Available: https://whatispiping.com/what-is-flow-induced-vibration/

[14] “(19) Role of Acoustic-Induced Vibration and Flow-Induced Vibration Studies in Oil & Gas Sector | LinkedIn.” Accessed: Jun. 12, 2024. [Online]. Available: https://www.linkedin.com/pulse/role-acoustic-induced-vibration-flow-induced-studies-oil-palanichamy/

[15] “Piping Vibration Analysis & Integrity Assessment | Vibration, dynamics and noise – Wood.” Accessed: Jun. 12, 2024. [Online]. Available: https://vdn.woodplc.com/services/piping-vibration-and-integrity-assessment/#a_1549

[16] J. La, J. Choi, S. Wang, K. Kim, and K. Park, “Continuous scanning laser Doppler vibrometer for mode shape analysis,” *https://doi.org/10.1117/1.1533794*, vol. 42, no. 3, pp. 730–737, Mar. 2003, doi: 10.1117/1.1533794.

[17] R. Parameshwaran, S. J. Dhulipalla, and D. R. Yendluri, “Fluid-structure Interactions and Flow Induced Vibrations: A Review,” in *Procedia Engineering*, Elsevier Ltd, 2016, pp. 1286–1293. doi: 10.1016/j.proeng.2016.05.124.

[18] P. Vasilyev and L. Fromzel, “AAnalytical Study of Piping Flow-induced Vibration.

Example of Implementation."
[19] D. K. S. a. P. J. Lee, "Material and thickness effects on flow-induced vibration in bent pipes," *J Press Vessel Technol*, vol. 138, 2016.
[20] X. D. Bai and W. Zhang, "Machine learning for vortex induced vibration in turbulent flow," *Comput Fluids*, vol. 235, p. 105266, Mar. 2022, doi: 10.1016/J.COMPFLUID.2021.105266.
[21] K. M. Holford, "Acoustic Emission–Basic Principles and Future Directions," *Strain*, vol. 36, no. 2, pp. 51–54, May 2000, doi: 10.1111/J.1475-1305.2000.TB01173.X.
[22] R. Parameshwaran, S. J. Dhulipalla, and D. R. Yendluri, "Fluid-structure Interactions and Flow Induced Vibrations: A Review," in *Procedia Engineering*, Elsevier Ltd, 2016, pp. 1286–1293. doi: 10.1016/j.proeng.2016.05.124.
[23] M. Paidoussis, "Fluid-Structure Interactions: Second Edition," *Fluid-Structure Interactions: Second Edition*, vol. 1, pp. 1–867, 2013, doi: 10.1016/C2011-0-08057-2.
[24] A. S. Tijsseling and P. Vaugrante, "FSI IN L-SHAPED AND T-SHAPED PIPE SYSTEMS." [Online]. Available: www.tue.nl/taverne
[25] J. S. Walker Associate Professor J W Phillips Associate Professor, "Pulse Propagation in FIuid-Filled Tubes," 1977. [Online]. Available: http://www.asme.org/about-asme/terms-of-use
[26] J. Gale and I. Tiselj, "Eight equation model for arbitrary shaped pipe conveying fluid," *Proceedings of the International Conference Nuclear Energy for New Europe 2006*, p. v, 2006, Accessed: Jun. 12, 2024. [Online]. Available: http://inis.iaea.org/Search/search.aspx?orig_q=RN:38115421
[27] H. Shen, J. Wen, D. Yu, and X. Wen, "The vibrational properties of a periodic composite pipe in 3D space," *J Sound Vib*, vol. 328, no. 1–2, pp. 57–70, Nov. 2009, doi: 10.1016/J.JSV.2009.07.032.
[28] D. M. Lee, M. J. Choi, and T. Y. Oh, "Transfer matrix modelling for the 3-dimensional vibration analysis of piping system containing fluid flow," *KSME Journal*, vol. 10, no. 2, pp. 180–189, Jun. 1996, doi: 10.1007/BF02953657/METRICS.
[29] Q. Zhao and Z. Sun, "Flow-induced vibration of curved pipe conveying fluid by a new transfer matrix method," *Engineering Applications of Computational Fluid Mechanics*, vol. 12, no. 1, pp. 780–790, Jan. 2018, doi: 10.1080/19942060.2018.1527725.
[30] F. K. Benra, H. J. Dohmen, J. Pei, S. Schuster, and B. Wan, "A comparison of one-way and two-way coupling methods for numerical analysis of fluid-structure interactions," *J Appl Math*, vol. 2011, 2011, doi: 10.1155/2011/853560.
[31] K. Haziq and I. Zaman, "Journal of Complex Flow Flow Induced Vibration Analysis in Pipeline by using One-Way and Two-Way Fluid Structure Interaction," *JCF Journal of Complex Flow*, vol. 5, no. 1, pp. 1–5, 2023, [Online]. Available: www.fazpublishing.com/jcf
[32] S. N, M. H, and F. S, "Study on vibration response of pipes induced by internal flow.," *ASME. PVP (American Society of Mechanical Engineers. Pressure Vessels and Piping Div.)*, vol. 189, pp. 233–238, 1990, Accessed: Jun. 13, 2024. [Online]. Available: https://jglobal.jst.go.jp/en/detail?JGLOBAL_ID=200902013246555571
[33] M. T. Pittard, "Large Eddy Simulation Based Turbulent Flow-induced Vibration of Fully Developed Pipe Flow BYU ScholarsArchive Citation," 2003. [Online]. Available: https://scholarsarchive.byu.edu/etd
[34] P. R. Resende, R. Roberto Frias, F. T. Pinho, and D. O. Cruz, "PERFORMANCE OF THE k-ε AND REYNOLDS STRESS MODELS IN TURBULENT FLOWS WITH VISCOELASTIC FLUIDS," 2006.
[35] S. Vijiapurapu and J. Cui, "Performance of turbulence models for flows through rough pipes," *Appl Math Model*, vol. 34, no. 6, pp. 1458–1466, Jun. 2010, doi:

10.1016/j.apm.2009.08.029.
[36] S. M. Salim, “Computational study of wind flow and pollutant dispersion near tree canopies.” [Online]. Available: https://www.researchgate.net/publication/255720118
[37] S. Salim M. and S. C. Cheah, “Wall Y Strategy for Dealing with Wall-bounded turbulent flows,” in *International MultiConference of Engineers and Computer Scientists*, 2009.
[38] A. A. Abuhatira, S. M. Salim, and J. B. Vorstius, “Numerical Simulation of Turbulent Pipe Flow With 90-Degree Elbow Using Wall Y+ Approach,” in *ASME International Mechanical Engineering Congress and Exposition, Proceedings (IMECE)*, American Society of Mechanical Engineers (ASME), 2021. doi: 10.1115/IMECE2021-69986.
[39] W. van Drongelen, “Signal processing for neuroscientists: An introduction to the analysis of physiological signals,” *Signal Processing for Neuroscientists: An Introduction to the Analysis of Physiological Signals*, pp. 1–308, Dec. 2006, doi: 10.1016/B978-0-12-370867-0.X5000-1.
[40] J. M. Cimbala, “Fourier Transforms, DFTs, and FFTs,” 2010.
[41] M. T. Pittard, R. P. Evans, R. D. Maynes, and J. D. Blotter, “Experimental and numerical investigation of turbulent flow induced pipe vibration in fully developed flow,” *Review of Scientific Instruments*, vol. 75, no. 7, pp. 2393–2401, Jul. 2004, doi: 10.1063/1.1763256.
[42] A. A. Abuhatira, S. M. Salim, and J. B. Vorstius, “CFD-FEA based model to predict leak-points in a 90-degree pipe elbow,” *Eng Comput*, vol. 39, no. 6, pp. 3941–3954, Dec. 2023, doi: 10.1007/s00366-023-01853-4.
[43] A. O. Ernest and O. A. David, “Boiler Efficiency Analysis of A 220mw Steam Power Plant Using Direct Method,” *International Journal of Research and Scientific Innovation*, vol. 09, no. 08, pp. 111–116, 2022, doi: 10.51244/ijrsi.2022.9802.
[44] H. Y. Ahmad, M. J. Jweeg, and D. C. Howard, “Prediction of the Resonance Frequency of the Pipe Carrying Fluid Relative to the Fluid Velocity,” 2023, pp. 363–372. doi: 10.1007/978-3-031-15758-5_36.